

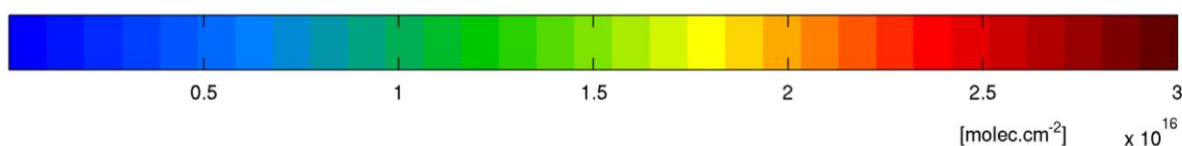
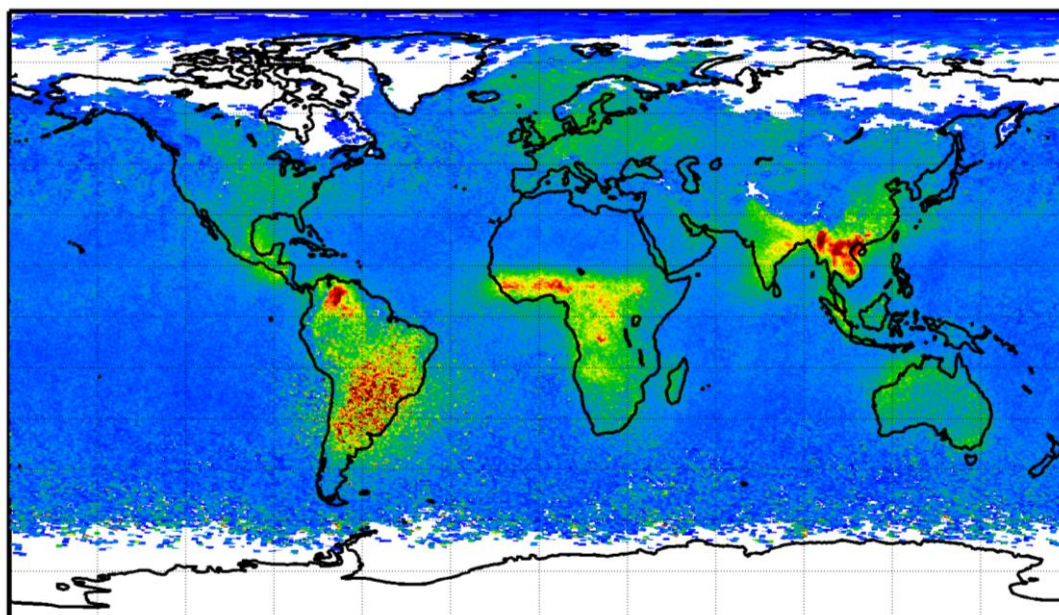
AC SAF ORR VALIDATION REPORT

Validated products:

Name	Acronym
Offline Total HCHO, GOME-2/MetOp-C	OTO/HCHO
NRT Total HCHO, GOME-2/MetOp-C	NTO/HCHO

DLR/EUMETSAT/BIRA-IASB
GDP 4.9

GOME-2/MetopC HCHO VCD April 2019



Authors:

Name	Institute
Gaia Pinaridi	Belgian Institute for Space Aeronomy
Huan Yu	Belgian Institute for Space Aeronomy
Michel Van Roozendael	Belgian Institute for Space Aeronomy
Jeroen van Gent	Belgian Institute for Space Aeronomy
Ka Lok Chan	German Aerospace Center
Pieter Valks	German Aerospace Center

Reporting period: February 2019 – July 2019

Input data versions: GOME-2 Level 1B version 6.3

Data processor versions: GDP 4.9, UPAS version 1.4.0

authors G. Pinardi, H. Yu, J. van Gent, M. Van Roozendael, K. Chan, and P. Valks
 edited by G. Pinardi, BIRA-IASB, Brussels, Belgium
 reference SAF/AC/IASB/VR/HCHO/TN-IASB-GOME2C-ACSAF-HCHO-2019
 document type AC SAF Validation Report
 issue 1
 revision 2
 date of issue 19 May 2020
 products MCG-O-HCHO, MCG-N-HCHO
 product version level-0-to-1 v6.3 , level-1-to-2 GDP v4.9

distribution

Function	Organisation
AC SAF	EUMETSAT, BIRA-IASB, DLR, DMI, DWD, FMI, HNMS/AUTH, KNMI, LATMOS, RMI
UPAS Team	DLR-IMF, DLR-DFD
Ground-based data providers	NIDFORVAL partners

external contributors

contributing ground-based correlative measurements from NIDFORVAL teams

Acronym	Organisation	Peoples
BIRA-IASB	Royal Belgian Institute for Space Aeronomy, Belgium	F..Hendrick, C. Vigouroux, M. Van Roozendael, M. de Mazière
MPIC	Max Planck Institute for Chemistry, Mainz, Germany	S. Donner, T. Wagner,
IFE/IUP	Institut für Umweltphysik/Fernerkundung, University of Bremen, Germany	M. Palm, J. Notholt
AUTH	Aristotle University of Thessaloniki, Thessaloniki, Greece	T. Drosoglou, A. Bais
UNAM	Centro de Ciencias de la Atmósfera, Universidad Nacional Autónoma de México, Mexico	C. Rivera, M. Grutter
CSCI	Instituto de Química Física Rocasolano, Madrid, Spain	A. Saiz-Lopez
UChiba	Center for Environmental Remote Sensing, Chiba University, Japan	H. Irie
FMI	Finnish Meteorological Institute, Sodankylä, Finland	R. Kivi
UPetersburg	Saint Petersburg State University, Atmospheric Physics Department, St. Petersburg, Russia	M. Makarova
UToronto	Department of Physics, University of Toronto, Canada	E. Lutsch, K. Strong
ULiege	Liège University, Belgium	E. Mahieu
NIWA	National Institute of Water and Atmospheric Research Ltd, New Zealand	D. Smale
KIT	Karlsruhe Institute of Technology, Garmisch-Partenkirchen, Germany	T. Blumenstock
UParis	Sorbonne University, Paris, France	Y. Te

document change record

Issue	Rev.	Date	Section	Description of Change
1	0	11.10.2019	all	Creation of this document
1	1	28/02/2020		Adding AC SAF product ID numbers table
1	2	19/05/2020	C	After ORR review

AC SAF product ID numbers

AC SAF internal identifier	Description
NRT Total HCHO	O3M-344
Offline Total HCHO	O3M-345

Validation report of GOME-2 GDP 4.9 HCHO column data for MetOp-C Operational Readiness Review

CONTENTS

ACRONYMS AND ABBREVIATIONS.....	4
INTRODUCTION TO EUMETSAT SATELLITE APPLICATION FACILITY ON ATMOSPHERIC COMPOSITION MONITORING (AC SAF).....	5
DATA DISCLAIMER FOR THE METOP-C GOME-2 TOTAL HCHO (OTO) DATA PRODUCTS.....	6
A. INTRODUCTION.....	8
A.1. Scope of this document.....	8
A.2. Preliminary remarks	8
A.3. Plan of this document	8
B. VALIDATION PROTOCOL.....	9
B.1. GDP 4.9 data and validation method.....	9
B.2. Reference data	10
C. VERIFICATION OF INDIVIDUAL COMPONENTS OF THE METOP-C GOME-2 PROCESSING CHAIN: METOP-C AGAINST METOP-B	12
C.1. Verification of Slant Column Density	12
C.2. Verification of Vertical Column Density	15
D. VERIFICATION OF INDIVIDUAL COMPONENTS OF PROCESSING CHAINS: TIME-SERIES ABOVE EMISSION REGIONS	18
E. COMPARISON WITH GROUND-BASED MEASUREMENTS	32
E.1. Ground-based correlative data.....	32
E.2. Validation method	32
E.3. Comparison with MAXDOAS	33
E.4. Comparison with FTIR.....	35
E.5. Conclusion on ground-based comparisons	39
F. CONCLUSIONS AND PERSPECTIVES.....	40
G. REFERENCES	41
G.1. Applicable documents	41
G.2. Reference.....	41
G.2.1 Peer-reviewed articles.....	41
G.2.2 Technical notes and presentations	43

ACRONYMS AND ABBREVIATIONS

AC SAF	Atmospheric Composition Monitoring Satellite Application Facility
AMF	Air Mass Factor, or optical enhancement factor
BIRA-IASB	Belgian Institute for Space Aeronomy
DLR	German Aerospace Centre
DOAS	Differential Optical Absorption Spectroscopy
Envisat	Environmental Satellite
ESA	European Space Agency
EUMETSAT	European Organisation for the Exploitation of Meteorological Satellites
FRM4DOAS	Fiducial Reference Measurements for Ground-Based DOAS Air-Quality Observations
FTIR	Fourier Transform Infrared Spectroscopy
GDP	GOME Data Processor
GEOMS	Generic Earth Observation Metadata Standard
GOME	Global Ozone Monitoring Experiment
HCHO	Formaldehyde
IMF	Remote Sensing Technology Institute
LOS	Line Of Sight
MAXDOAS	Multi Axis Differential Optical Absorption Spectroscopy
MPC	Mission Performance Center
NDACC	Network for the Detection of Atmospheric Composition Change
NIDFORVAL	S5P Nitrogen Dioxide and FORmaldehyde Validation using NDACC and complementary FTIR and UV-Vis DOAS ground-based remote sensing data
O ₃	Ozone
OCRA	Optical Cloud Recognition Algorithm
OMI	Ozone Monitoring Instrument
QA4ECV	Quality Assurance for Essential Climate Variables
ROCINN	Retrieval of Cloud Information using Neural Networks
RRS	Rotational Raman Scattering
RTS	RT Solutions Inc.
SCD	Slant Column Density
SCIAMACHY	Scanning Imaging Absorption spectroMeter for Atmospheric CHartography
SNR	Signal to Noise Ratio
SZA	Solar Zenith Angle
TEMIS	Tropospheric Emission Monitoring Internet Service
TROPOMI	TROPOspheric Monitoring Instrument
UPAS	Universal Processor for UV/VIS Atmospheric Spectrometers
UVVIS	Ultraviolet-visible spectrometry
VCD	Vertical Column Density
WMO	World Meteorological Organization

INTRODUCTION TO EUMETSAT SATELLITE APPLICATION FACILITY ON ATMOSPHERIC COMPOSITION MONITORING (AC SAF)

Background

The monitoring of atmospheric chemistry is essential due to several human caused changes in the atmosphere, like global warming, loss of stratospheric ozone, increasing UV radiation, and pollution. Furthermore, the monitoring is used to react to the threats caused by the natural hazards as well as follow the effects of the international protocols.

Therefore, monitoring the chemical composition and radiation of the atmosphere is a very important duty for EUMETSAT and the target is to provide information for policy makers, scientists and general public.

Objectives

The main objectives of the AC SAF is to process, archive, validate and disseminate atmospheric composition products (O₃, NO₂, SO₂, BrO, HCHO, H₂O, OClO, CO, NH₃), aerosol products and surface ultraviolet radiation products utilising the satellites of EUMETSAT. The majority of the AC SAF products are based on data from the GOME-2 and IASI instruments onboard Metop satellites.

Another important task besides the near real-time (NRT) and offline data dissemination is the provision of long-term, high-quality atmospheric composition products resulting from reprocessing activities.

Product categories, timeliness and dissemination

NRT products are available in less than three hours after measurement. These products are disseminated via EUMETCast, WMO GTS or internet.

- Near real-time trace gas columns (total and tropospheric O₃ and NO₂, total SO₂, total HCHO, CO) and high-resolution ozone profiles
- Near real-time absorbing aerosol indexes from main science channels and polarization measurement detectors
- Near real-time UV indexes, clear-sky and cloud-corrected

Offline products are available within two weeks after measurement and disseminated via dedicated web services at EUMETSAT and AC SAF.

- Offline trace gas columns (total and tropospheric O₃ and NO₂, total SO₂, total BrO, total HCHO, total H₂O) and high-resolution ozone profiles
- Offline absorbing aerosol indexes from main science channels and polarization measurement detectors
- Offline surface UV, daily doses and daily maximum values with several weighting functions

Data records are available after reprocessing activities from the EUMETSAT Data Centre and/or the AC SAF archives.

- Data records generated in reprocessing
- Lambertian-equivalent reflectivity
- Total OClO

Users can access the AC SAF offline products and data records (free of charge) by registering at the AC SAF web site.

More information about the AC SAF project, products and services: <https://acsaf.org/>

AC SAF Helpdesk: helpdesk@acsaf.org

Twitter: https://twitter.com/Atmospheric_SAF

DATA DISCLAIMER FOR THE METOP-C GOME-2 TOTAL HCHO (OTO) DATA PRODUCTS

In the framework of EUMETSAT's Atmospheric Composition Monitoring Satellite Application Facility (ACSAF), GOME-2 formaldehyde (HCHO) total column data product are generated at DLR from MetOp-C GOME-2 measurements using the UPAS environment version 1.4.0 the level-0-to-1 v6.3 processor and the level-1-to-2 GDP v4.9 DOAS retrieval processor (see TN-DLR-ATBD and TN-DLR-PUM). BIRA-IASB and DLR ensure detailed quality assessment of algorithm upgrades and continuous monitoring of GOME-2 HCHO data quality with a recurring geophysical validation using correlative measurements from ground-based instruments and from other satellites, modelling support, and independent retrievals.

This report presents the initial verification of MetOp-C GOME-2 HCHO column data (OTO) recorded from February to July 2019. GDP 4.9 HCHO column data are investigated through:

- (1) verification of the consistency of GDP4.9 GOME-2C column retrievals against operational GOME-2B data sets, for the different steps contributing to the VCD;
- (2) evaluation of the HCHO vertical column against ground-based observations provided MAXDOAS and FTIR spectrometers.

The main results from the verification are summarized hereafter:

1. The current quality of the MetOp-C GOME-2 radiance and irradiance spectra in the 328.5-346 nm spectral interval enables HCHO slant column retrievals. However, a viewing geometry dependence is found in GOME-2C SCD and SCDcorrected, that is transferred in the VCD, leading to a large number of negative columns for large off-nadir scan angles. This dependence might be due to polarisation-related spectral features in the level-1 data.
2. GOME-2C HCHO fit residuals and scatter on the slant column are systematic smaller than for GOME-2B, in a range from 20% in tropical to 50% over high latitudes, but are generally comparable to those obtained from Metop-B spectra at beginning of operations. GOME-2C slant columns show a slightly higher bias compared to GOME-2B.
3. A smaller signature of the SAA is found for GOME-2C compared to MetopB.
4. GOME-2C VCD are about ~71% larger than GOME-2B for the pixels between 70°S and 70°N, with VCD values exceeding 10^{15} molecules/cm², and excluding the SAA regions. If only pixels exceeding 6×10^{15} molecules/cm² VCD are considered, the average difference is within 32%. In the explored emissions regions, the temporal evolution of GOME-2C is similar to GOME-2B, with GOME-2C being generally a few % larger than GOME-2B in emission regions (up to 15% in average over Southern China), while in regions with low HCHO, GOME-2C is slightly smaller (Pacific and Europe in winter time).

In average, these differences meet the accuracy requirement of HCHO for polluted cases (50%), and are very close to the optimal requirement (30%).

5. Gathering of preliminary HCHO columns from ground-based MAXDOAS (9 stations) and 14 FTIR stations within the NIDFORVAL project allowed a first validation of the GOME-2C and GOME-2B vertical columns. Differences in the daily comparisons (both for MAXDOAS and FTIR data) are found for GOME-2C compared to results with GOME-2B, with a larger daily spread in the first case (with a larger number of large negative columns), as already pointed out in the verification section. The impact of the large GOME-2C spread values is reduced in the monthly mean comparisons and similar results are found for the MAXDOAS comparisons, while larger differences are found for the FTIR case. Slope of 0.56 wrt smoothed FTIR values are found for GOME-2C, compared to 0.94 with GOME-2B. Validation results present a relatively good

agreement, but the FTIR comparisons over 6 months are at the limit of the 50% threshold requirement for GOME-2C.

A. INTRODUCTION

A.1. Scope of this document

The present document reports on the verification and preliminary geophysical validation of GOME-2/MetOp-C HCHO column data acquired over the February-July 2019 time period. The data are produced by the GOME Data Processor (GDP) v4.9 operated at the DLR Remote Sensing Technology Institute (DLR-IMF, Oberpfaffenhofen, Germany) in the framework of the EUMETSAT AC SAF. This report concentrates on comparisons of GOME-2/Metop-C data with GOME-2/Metop-B GDP 4.8 (the current operational version for Metop-A and B) and with correlative observations acquired by independent ground-based spectrometers. The goal is to investigate the consistency of the GOME-2C HCHO columns and if the product fulfil the user requirements in term of accuracy, as defined in the (threshold 100%, target 50% (polluted) and optimal 30%) %), as stated in the ACSAF Service Specification Document (https://acsaf.org/docs/AC_SAF_Service_Specification.pdf).

A.2. Preliminary remarks

To report on the status of the verification of the MetOp-C GOME-2 HCHO columns, in addition to comparisons against GOME-2 on MetOp-B, the consistency of the different HCHO products is explored by performing comparisons with available correlative data sets. As discussed in detail in Section B2, it should be noted that this part rely on the early delivery of partners within other validation projects (e.g. NIDFORVAL). Results relying on early-delivery data must always be considered as preliminary and more firm conclusions on validation should be updated in the future, to be assembled when more Metop-C measurements will be available (ideally covering at least one year of data). Moreover, several improvements on the HCHO product itself have been suggested in the past, but these are out of the scope of the present document.

A.3. Plan of this document

After presentation of the AC SAF introduction and the GOME-2 Data Disclaimer for HCHO column products, this document is divided into the following sections:

- A. Introduction
- B. Validation Protocol
- C. Step by step verification: METOP-C against METOP-B GOME-2 HCHO operational retrievals.
- D. Step by step verification: Time-series above emission regions.
- E. Validation against ground-based MAXDOAS and FTIR data
- F. Conclusion
- G. References

B. VALIDATION PROTOCOL

B.1. GDP 4.9 data and validation method

Retrieval principles of GOME-2C HCHO data are described in the Algorithm Theoretical Basis Document (ATBD, 2017) and the Product User Manual (PUM, 2017) available via the AC SAF web site (<https://acsaf.org>). Validation method was set up for the validation of GOME-2A and GOME-2B, and we refer to the last HCHO validation report (AC SAF VR 2015). This document is based on the same method, but with a more specific focus on establishing the verification and validation of the GOME-2C GDP 4.9 HCHO data, by checking the consistency between the GOME-2C and GOME-2B product over the 6 months dataset available and providing preliminary validation results with correlative ground-based data.

The latest GOME Data Processor (GDP) for MetOp-C is called version 4.9 due to major changes in the SO₂ product, but only minor changes have been implemented for the HCHO operational product (see Table B.1). The processor is coherent with processor GDP 4.8 operational for MetOp-A/B data. Since GDP 4.8, two inter-linked fitting intervals (332-359 nm for BrO, 328.5-346 nm for HCHO) have been implemented to reduce the scatter on HCHO slant columns, as summarized in Table B.1. To reduce the impact of remaining unresolved spectral artefacts, an absolute normalization is applied on a daily basis using the reference sector method over the Pacific Ocean (Longitude: 140°-160° W), where the only source of HCHO is CH₄ oxidation. The mean HCHO slant column density in the reference sector is subtracted from the retrieved slant columns on this day ($\Delta S = S - S_0$), and replaced by a HCHO background value (V_0^{CTM}) taken from the tropospheric 3-D chemistry transport model IMAGESv2 (Mueller and Stavrou, 2005) results:

$$V = \Delta S/M + V_0^{\text{CTM}}$$

where M is the air-mass factor calculated with a priori HCHO profiles coming from IMAGESv2 for the year 2007, surface albedo from the combined TOMS/GOME climatology (Boersma et al., 2004), and cloud information from OCRA-ROCINN (Lutz et al., 2016). Averaging kernels are also provided. Only slight adaptations in the DOAS fitting have been included for GOME-2C, such as accounting for the different GOME-2/FM2 slit function and including a pseudo-cross section to account for changes in resolution (see table B.1).

Table B.1: Summary of DOAS settings for GOME-2A and GOME-2B (GDP 4.8) and GOME-2C (GDP 4.9)

	GOME-2A and GOME-2B (GDP 4.8)
Calibration	SAO2010 (Chance&Kurucz, 2010)
Slit function	FM203(GOME-2A)/FM202(GOME-2B) from GOME-2 calibration key data (EUMETSAT, 2009)
Polynomial	5 th order
Intensity offset	linearized (inversed earth-shine)
H₂CO	Meller&Moortgat, 2000
O₃	Brion et al., 1998/Malicat et al. 1995
BrO	Fleischmann et al., 2004
NO₂	Vandaele et al., 2002
OCIO	Bogumil et al., 2003
Ring effect	2 ring cross sections calculated using SCIATRAN (Rozanov et al., 2001)

Polarisation vectors	Eta/Zeta GOME-2 calibration key data (EUMETSAT, 2009)
Non-linear O₃ absorption effects	2 pseudo cross sections from Taylor expansion of wavelength and optical depth (Puķīte et al., 2010)
Fitting interval 1	332-359 nm
Included cross sections	H ₂ CO(298K), NO ₂ (220K), OCIO(293K), O ₃ (228K/243K), 2 pseudo cross sections (O ₃ O ₃ /λO ₃), Zeta/Eta, Ring1/Ring2, BrO(223K)
Fitting interval 2	328.5-346 nm
Included cross sections	H ₂ CO(298K), NO ₂ (220K), OCIO(293K), O ₃ (228K/243K), 2 pseudo cross sections (O ₃ O ₃ /λO ₃), Zeta/Eta, Ring1/Ring2 <i>BrO (from fitting interval 1)</i>
Specificities for GOME-2C (GDP 4.9)	Inclusion of a resolution pseudo cross-section in the DOAS fit; Slit function: FM201(GOME-2C) from GOME-2C calibration key data (EUMETSAT, 2018)

We follow a validation protocol that consists in a step-by-step verification of each sub-product:

- slant columns (SCD)
- normalized slant columns (Δ SCD) (see [ATBD] and De Smedt et al., 2008 for more details about the reference sector correction)
- air mass factors without cloud correction (AMF_{clear})
- air mass factors with independent pixel cloud correction (AMF)
- total vertical columns (VCD) (the bulk of the formaldehyde column lies in the lower troposphere, the contribution from the stratosphere is negligible).

The total vertical columns are then compared with correlative ground-based measurements, such as MAXDOAS and FTIR data.

B.2. Reference data

The AC SAF GDP HCHO operational product is the only product providing recent data for GOME-2, as no scientific product is continuously maintained or adapted for GOME-2B or GOME-2C to our knowledge. GOME-2 products such as the BIRA/TEMIS data (Sc.v12, Sc.v14, De Smedt et al., 2008; 2010; 2012; 2015, <http://h2co.aeronomie.be/>) or the QA4ECV dataset (De Smedt et al., 2018, <http://www.qa4ecv.eu/ecv/hcho-p/data>) only covers up to 2016. Existing TROPOMI and OMI HCHO data have an overpass in the early afternoon. So only satellite-to-satellite comparisons among AC SAF operational products for the different MetOp is performed here.

GOME-2B and GOME-2C HCHO VCDs are compared to correlative ground-based observations, as done in the previous Validation Report for GDP 4.8 (AC SAF VR 2015). Due to instrumental failures, the number of BIRA-IASB currently operating MAXDOAS instruments is limited (for the GOME-2C received period February to July 2019, only Uccle and Reunion-Maido instruments were measuring). The comparisons have been extended to ground-based data collected by BIRA from different partners in the context of the NIDFORVAL project (S5P Nitrogen Dioxide and FORmaldehyde Validation using NDACC

and complementary FTIR and UV-Vis DOAS ground-based remote sensing data). This ESA AO project aims at creating and collecting ground-based datasets from NDACC and complementary networks, to be used in the validation of TROPOMI data. FTIR HCHO harmonized retrievals settings have been defined (with uncertainty budget and averaging kernels) and generated at more than 20 FTIR stations (Vigouroux et al., 2018). MAXDOAS data have been gathered at 9 stations from existing datasets (mostly based on recommended settings) and preliminary processing coming from the ongoing set-up of the FRM4DOAS centralized processing. These datasets covers a wide range of HCHO levels, from artic, antarctic, oceanic, mountainous remote levels to polluted conditions. Most of the stations have provided recent data, which are used for the TROPOMI HCHO product validation (e.g., Vigouroux et al., 2019), and are used in Section E for the GOME-2 GDP products.

C. VERIFICATION OF INDIVIDUAL COMPONENTS OF THE METOP-C GOME-2 PROCESSING CHAIN: METOP-C AGAINST METOP-B

C.1. Verification of Slant Column Density

To test the quality of the DOAS HCHO slant column fit on GOME2-C spectra, GDP has been used to retrieve HCHO slant column amounts from spectra recorded along a single orbit of GOME-2 Metop-C (orbit #1535, February 23, 2019), and of GOME-2 Metop-B in 2019 (orbit #33378, February 23, 2019). Current version of GDP product for GOME-2 Metop-B and -C are 4.8 and 4.9, respectively.

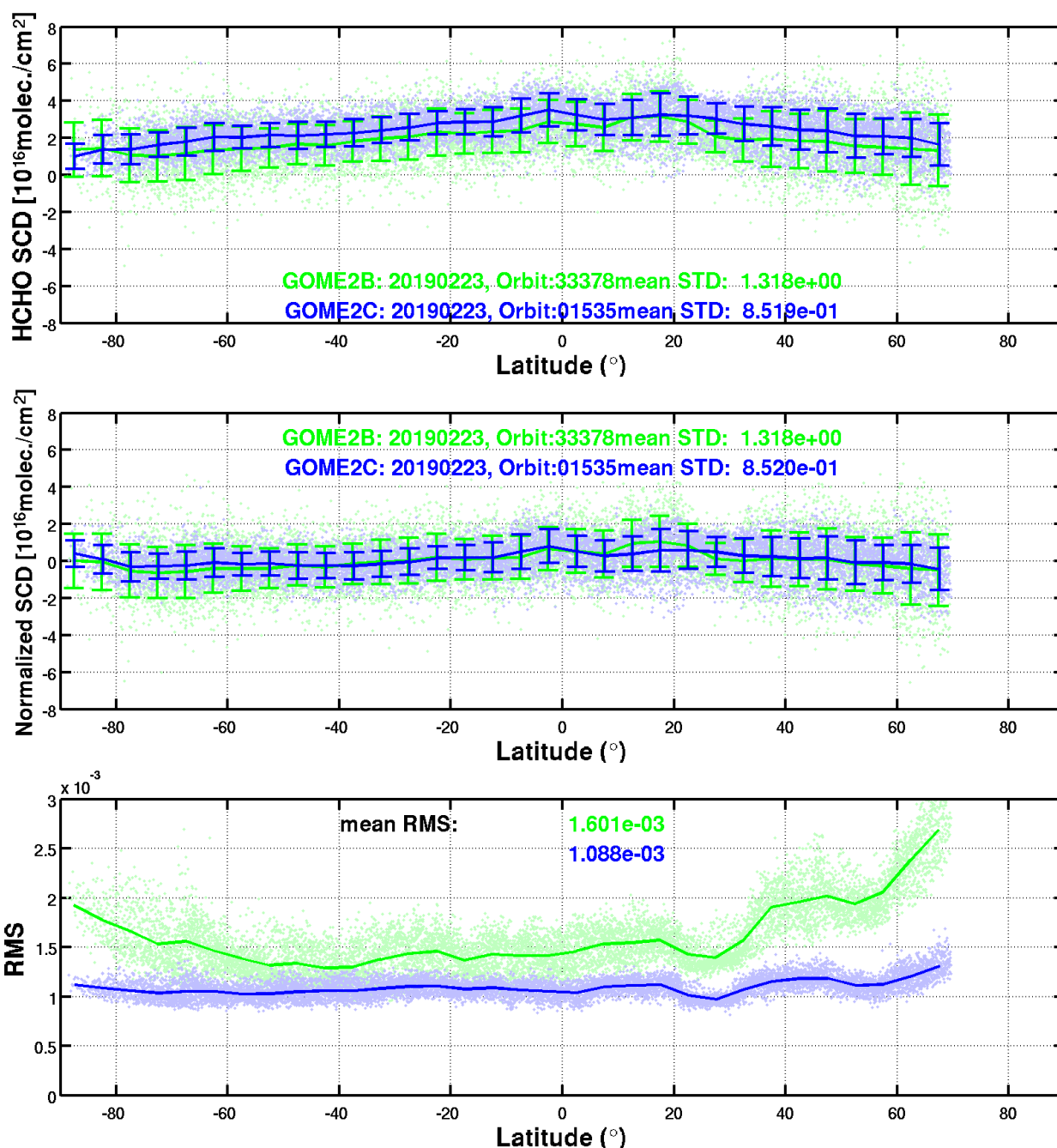


Figure C.1.1: HCHO retrievals for one orbit of GOME-2 on METOP-B (green, 23/02/2019, orbit nb. 33378) and METOP-C (blue, 23/02/2019, orbit nb. 1535) in 2019. Dots are individual measurements; lines are averages within 5° latitude-bands. First panel: slant columns and standard deviation of the slant columns within the 5° latitude-bands (STD), second panel: normalized slant columns and standard deviation, third panel: residuals of the fit (RMS).

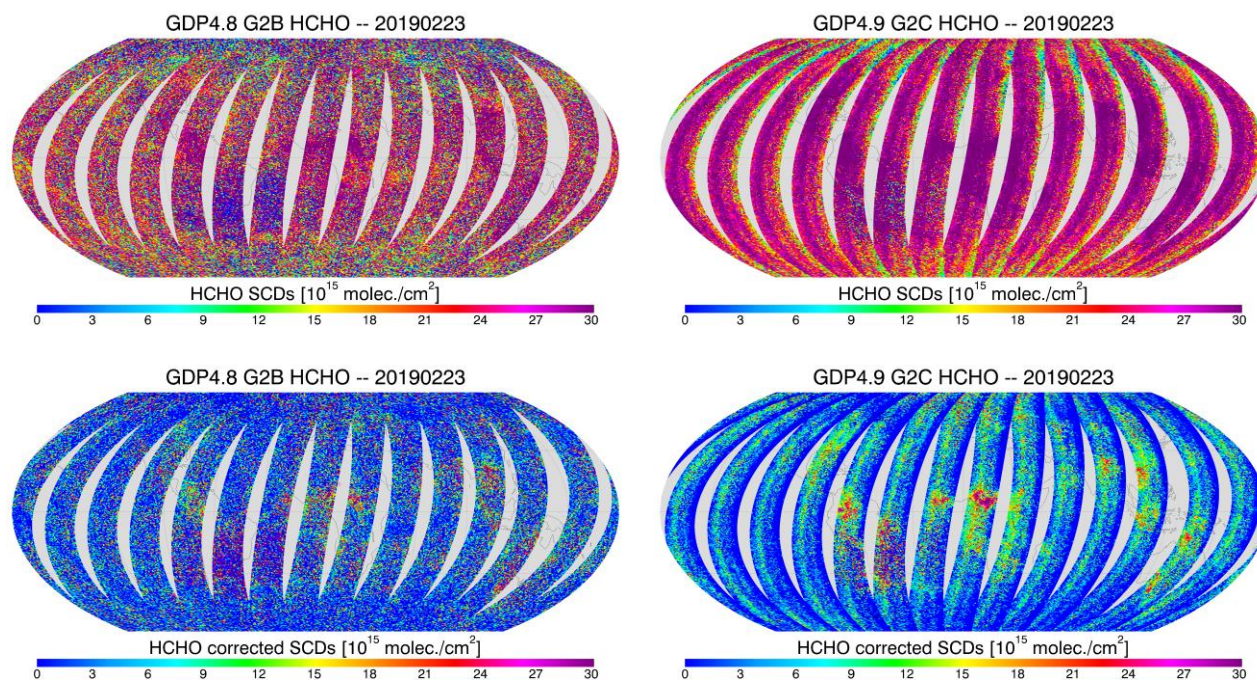


Figure C.1.2: Maps of slant columns (upper panel) and normalized slant columns (bottom panel) on 23rd February 2019, obtained from GDP 4.8 GOME-2B (left panel) and GDP4.9 GOME-2C (right panel) products.

From inspection of Figures C.1.1 and C.1.2, we can conclude the following:

- Raw HCHO slant columns (before the reference sector correction) derived from GOME-2B GDP4.8 and GOME-2C GDP 4.9 are generally consistent, although GOME-2C slant columns show slightly higher bias.
- After application of the reference sector correction, normalized HCHO slant columns between two products shows generally good agreement. Map of GOME2-2C slant columns however presents a viewing geometry dependence, with higher values in nadir and lower values at large off-nadir scan angle, which is not present in GOME-2B.
- The scatter of the slant columns and the fitting residual for GOME-2B are systematic higher than for GOME-2C, range from 20% in tropical to 50% over high latitudes.

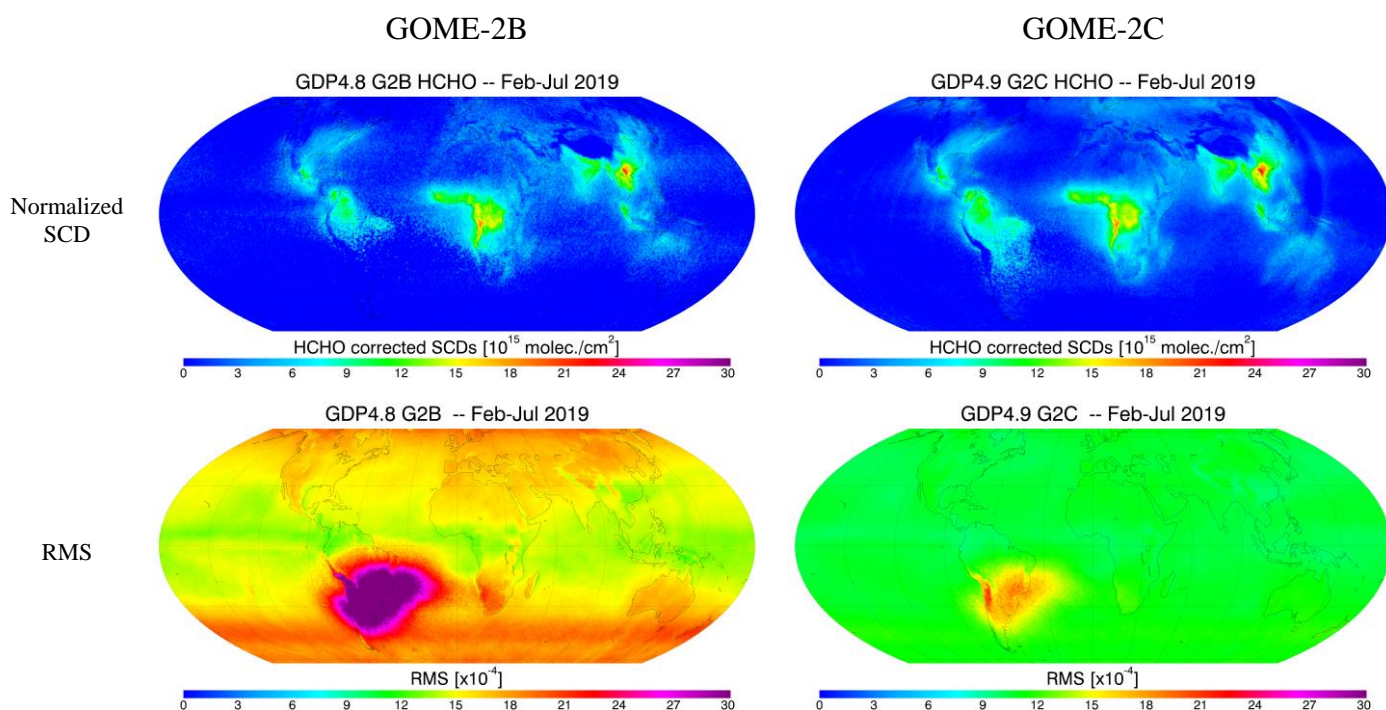


Table C.1.3: Maps of averaged normalized slant columns (with the reference sector correction), and fitting residuals from February to July 2019, obtained from GOME-2B GDP 4.8 and GOME-2C GDP4.9 products. Note that, no cloud filter is applied in this cases.

G2B GDP4.8 - G2C GDP4.9 -- Feb-Jul 2019

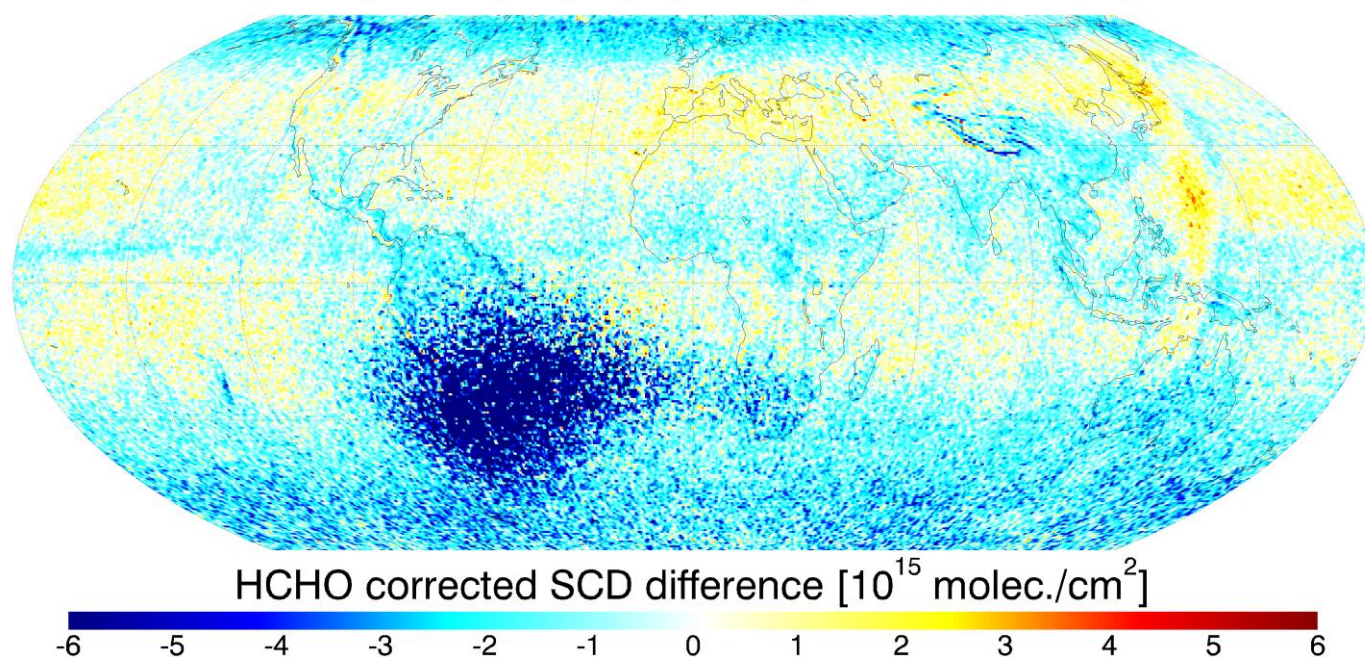


Figure C.1.4: Map of averaged normalized slant column density differences between GOME-2B GDP4.8 and GOME-2C GDP4.9, obtained from February to July 2019.

Monthly averaged maps of normalized slant columns (Figure C.1.3) derived from GOME-2B and GOME-2C also show a high degree of consistency. However, some differences are visible in a few areas (Figure

C.1.4). The largest different is over the South American Anomaly (SAA) region, since the spike removing approach is not implemented in the current GDP product, and this will introduce a large error in HCHO retrieval.

There is a positive bias between 120°E and 150°E, probably due to viewing geometric dependency issue in GOME-2C product. In addition, a systematic negative bias is found over high latitudes.

Apart from SAA region, maps of fitting residuals (RMS) from GOME-2B varies from $\sim 1.5 \times 10^{-3}$ at tropical region to $\sim 2.1 \times 10^{-3}$ at large SZA, and RMS is slightly larger over South Hemisphere than over North Hemisphere. Whereas, RMS from GOME-2C is $\sim 1.2 \times 10^{-3}$ globally.

C.2 Verification of Vertical Column Density

This section concentrates on the verification of the HCHO vertical column densities. Figure C.2.1 and C.2.2 illustrate the status of the comparisons between GDP4.8 applied to GOME-2B and GDP4.9 applied to GOME-2C. For the verification, the pixels with intensity-weighted cloud fraction $> 50\%$ and surface albedo > 0.3 are discarded to control the quality of the retrieved data.

Good agreement between GDP 4.8 GOME-2B and GDP 4.9 GOME-2C is found for both tropospheric vertical column and tropospheric air mass factor, even over the polluted region. The GOME-2B data over 75°S-80°S and 25°N-30°N for orbit 33378 is missing (Figure C.2.1 and Figure C.2.2) because of the cloud coverage, and GOME-2C only have a few valid measurements as well.

Global average maps (Figure C.2.3) show similar result as the orbit data, which has a high degree of consistency between GOME-2B and GOME-2C products. Viewing angle dependency is almost smoothed by the average. Some differences are linked to the differences in the slant column density (Figure C.1.4).

Based on the monthly averaged maps (gridded at $0.5^\circ \times 0.5^\circ$) from February to July 2019, the difference in vertical column density between GOME-2B and GOME-2C is $\sim 71\%$ for the pixels with VCD values exceed 10^{15} molecules/cm², between 70°S and 70°N, and excluding the SAA regions. If only the pixels with VCD exceed 6×10^{15} molecules/cm² are considered, the average difference is within 32% between GOME-2B and GOME-2C. It meets the accuracy requirement of HCHO for polluted cases (50%), very close to the optimal requirement (30%).

The averaged AMF maps is highly consistent between GOME-2B and GOME-2C, the small bias can be found over land region, especially over Sahara Desert, which is probably due to an issue for the background albedo map in cloud retrieval. GOME-2B and GOME-2C uses the same 'clear-sky reflectance composite map' dataset in OCRA cloud retrieval, since the GOME-2C background dataset is not available right now. In addition, the scan angle dependency might also play a role in the cloud retrieval. Cloud fraction product could clearly see the difference between GOME-2B and GOME-2C, GOME-2B map sees more cloudy than GOME-2C over this region (Figure C.2.4). Difference in the surface albedo will affect the retrieval of cloud properties, and then affect the calculation of the HCHO AMF. In addition, the retrieved cloud fraction will affect the data selection in the average maps.

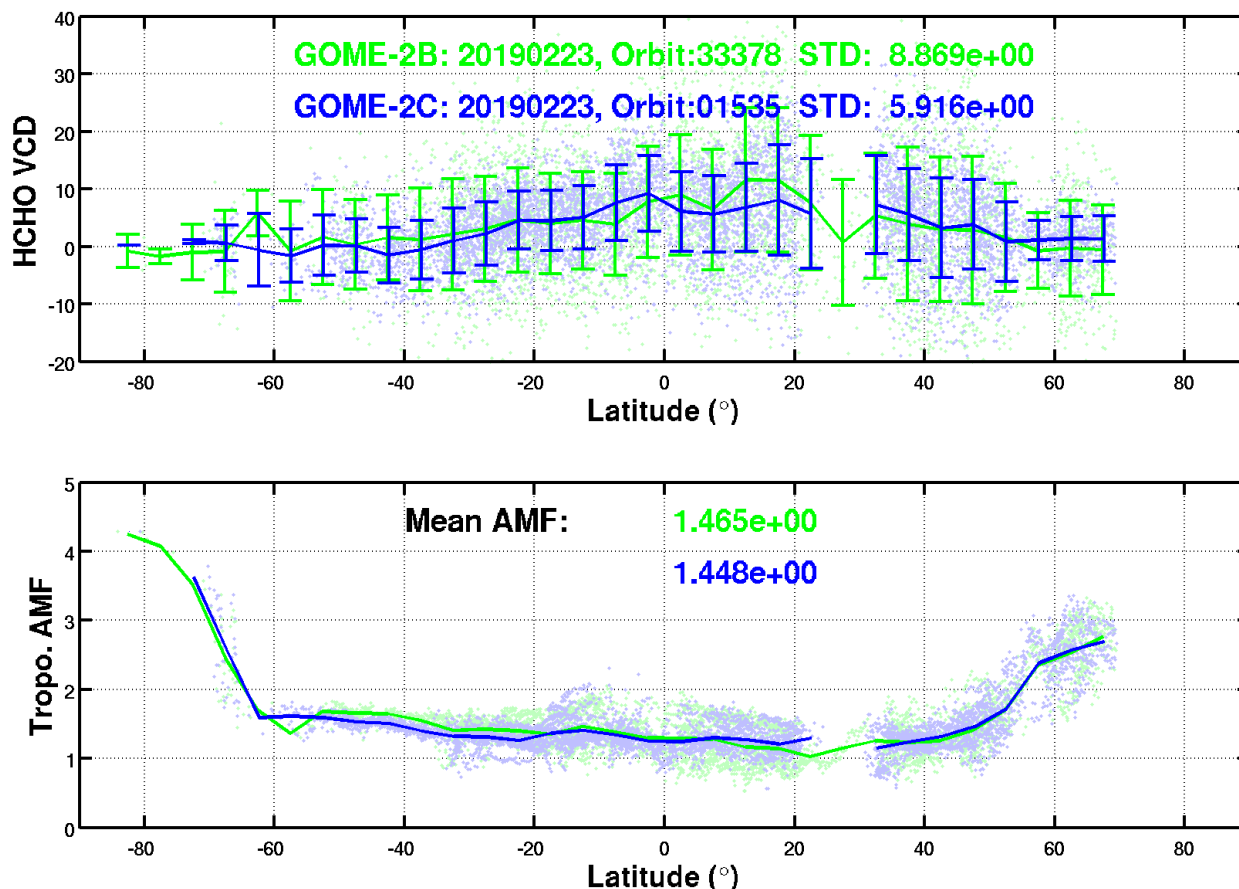


Figure C.2.1: HCHO retrievals for one orbit of GOME-2 on METOP-B (green, 23/02/2019, orbit nb. 33378) and METOP-C (blue, 23/02/2019, orbit nb. 1535) in 2019. Dots are individual measurements; lines are averages within 5° latitude-bands. First panel: slant columns and standard deviation of the slant columns within the 5° latitude-bands (STD), second and third panel are tropospheric air mass factor. Only the valid HCHO retrieval with intensity-weighted cloud fraction less than 50% and surface albedo less than 0.3 are used.

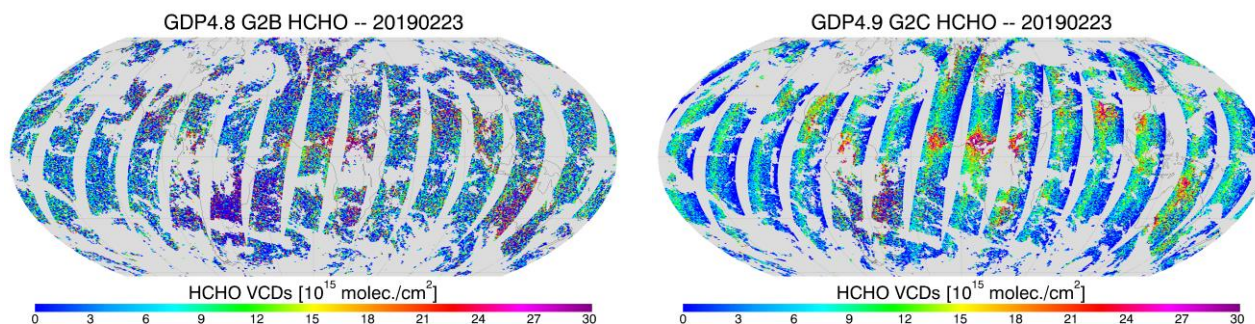


Figure C.2.2: Maps of HCHO tropospheric vertical columns on 23rd February 2019, obtained from GOME-2B GDP 4.8 (left panel) and GOME-2C GDP4.9 (right panel) products.

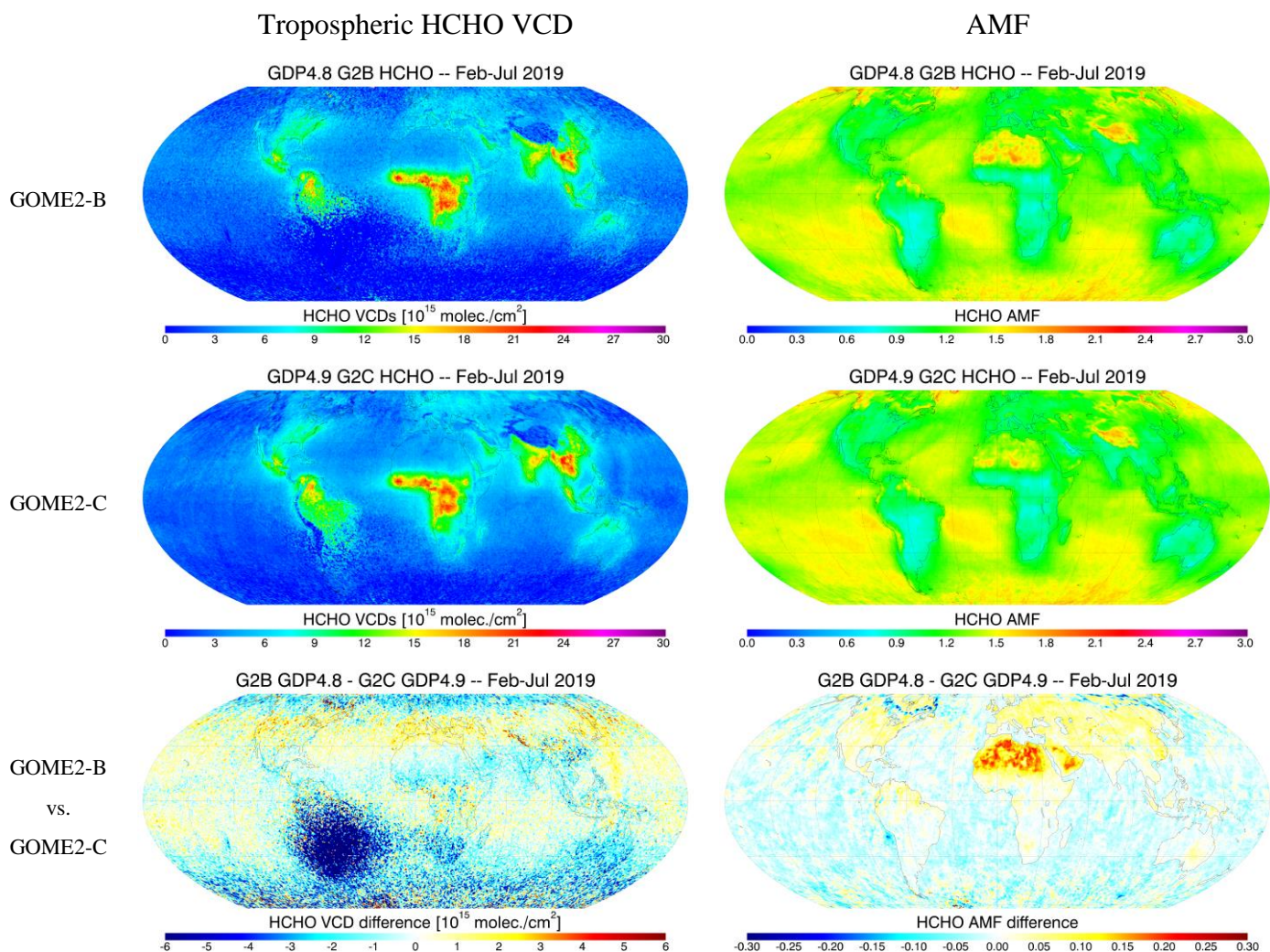


Figure C.2.3: Maps of averaged tropospheric vertical columns and tropospheric air mass factor, obtained from GDP 4.8 GOME-2B and GDP4.9 GOME-2C cloud- and snow-free (intensity-weighted cloud fraction < 50% and surface albedo < 0.3) measurements from February to July 2019, and their differences.

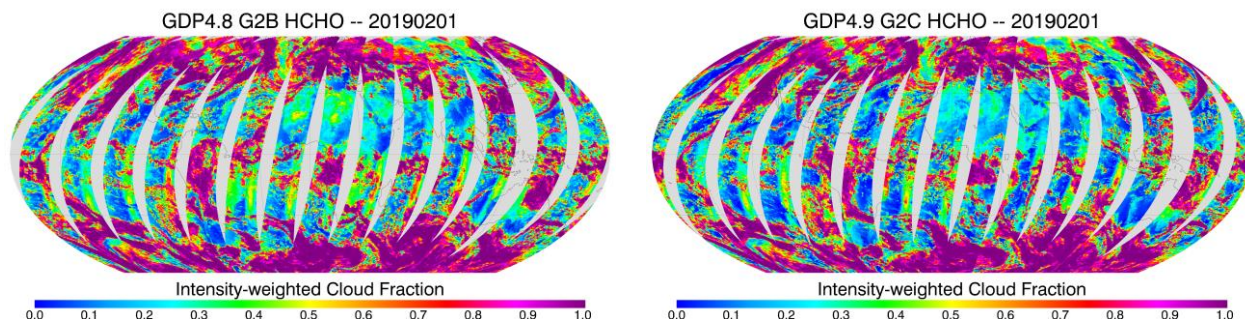


Figure C.2.4: Maps of intensity-weighted cloud fraction for GOME-2B (left) and GOME-2C (Right) on 1st February 2019.

D. VERIFICATION OF INDIVIDUAL COMPONENTS OF PROCESSING CHAINS: TIME-SERIES ABOVE EMISSION REGIONS

In this section, time-series of GOME-2A, GOME-2B and GOME-2C operational HCHO data products are presented for a selection of emission regions (listed in Table D.1), for 2019. The individual components of the HCHO VCD processing chain are compared separately, in order to visualize possible compensating differences.

Table D.1: List of the emissions regions considered for the comparisons.

Region	Lat Min	Lat Max	Long Min	Long Max
Northern_Australia	-19	-10	123	145
Northern_China	29	37	112	121
India	15	24	75	85
South_Asia	12	22	98.5	110
Indonesia	-5	5	98	118
Northern_Africa	3	14	-14	12
Equatorial_Africa	-5	8	14	28
Southern_Africa	-15	-5	10	30
Southeastern_US	30	40	-95	-75
Guatemala	12.5	17.5	-95	-85
Mexico	15	20	-103	-88
Amazonia	-10	5	-75	-50

Figures D.1 to D.12 presents the time-series of monthly mean values of several HCHO-related parameters, such as:

- The tropospheric vertical column (VCD) (the DETAILED_RESULTS/HCHO/VCD_corrected in the hdf file)
- The normalized slant column (Δ SCD) (the DETAILED_RESULTS/HCHO/ESCcorrected in the hdf file)
- The clear-sky air mass factor (AMFclear) and the cloud-corrected (total tropospheric) air mass factor (AMF).
- The DOAS fit RMS, which is a good indicator of the fit quality.
- The standard deviation of the slant columns (sigmaSCD), as an indicator of the noise on the slant columns

Satellite HCHO VCD means are calculated using all pixels falling within the region boundaries and meeting the following selection criteria:

- slant column densities (SCDs) larger than -4×10^{16} molec/cm², RMS lower than 3×10^{-3} ; solar zenith angle (SZA) lower than 70°, and cloud fraction lower than 40%.
- The monthly mean for the regions is performed if there are at least 500 points > 500, SZA <= 60, Cloud fractions <= 0,4

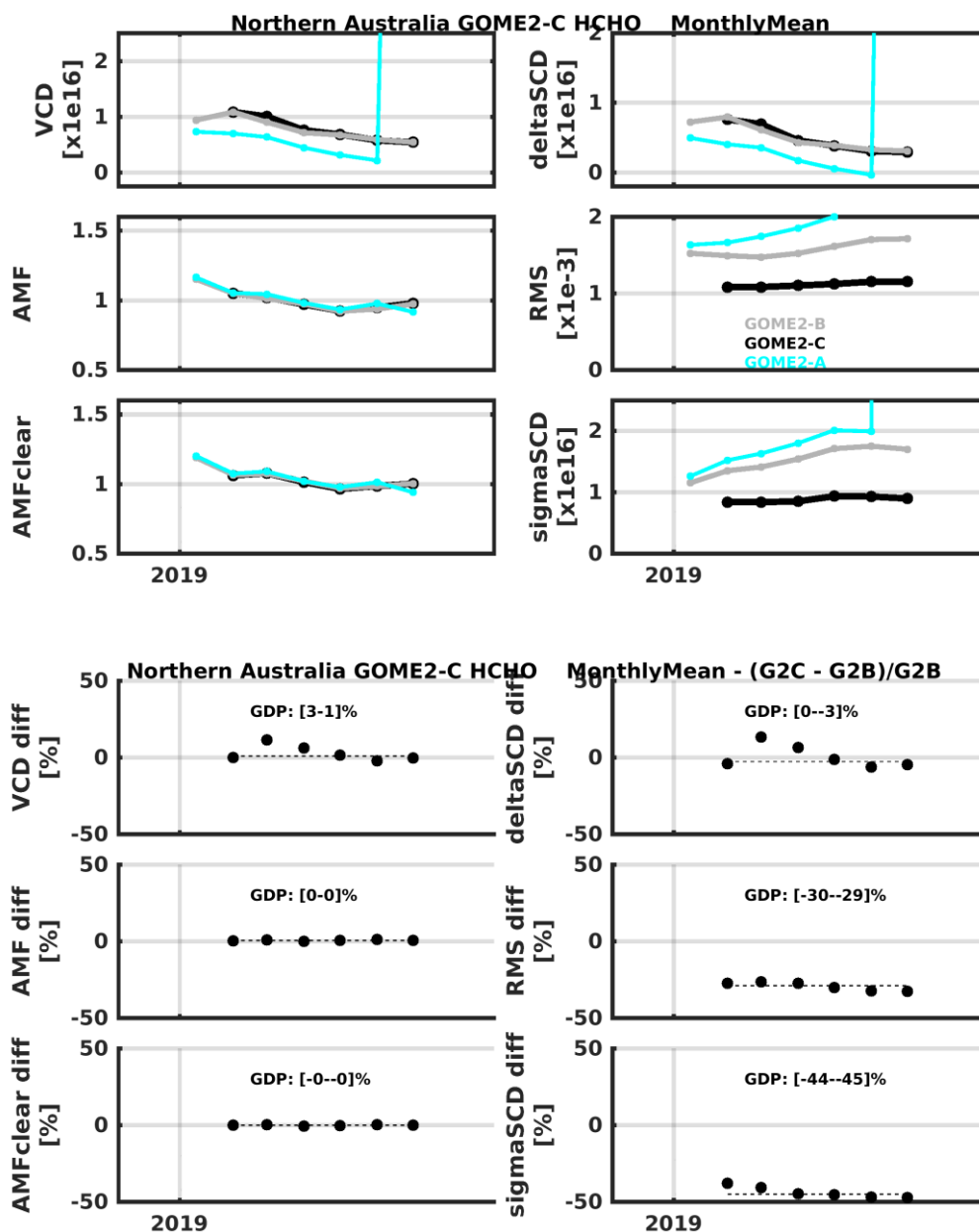


Figure D.1: Upper panel: GOME-2C GDP-4.9 (black), GOME-2B (grey) and GOME-2A (cyan) GDP-4.8 HCHO comparison in 2019 in the Northern Australian region. The different panels present HCHO vertical columns (VCD), the normalized slant columns (deltaSCD), the residuals of the fit (RMS), the total air mass factors (AMF) and the clear-sky air mass factors (AMFclear) and the standard deviation of the slant columns (sigmaSCD). Lower panel: Relative differences between the GOME-2C and GOME-2B products. Numbers inset are the mean and median differences over the time series.

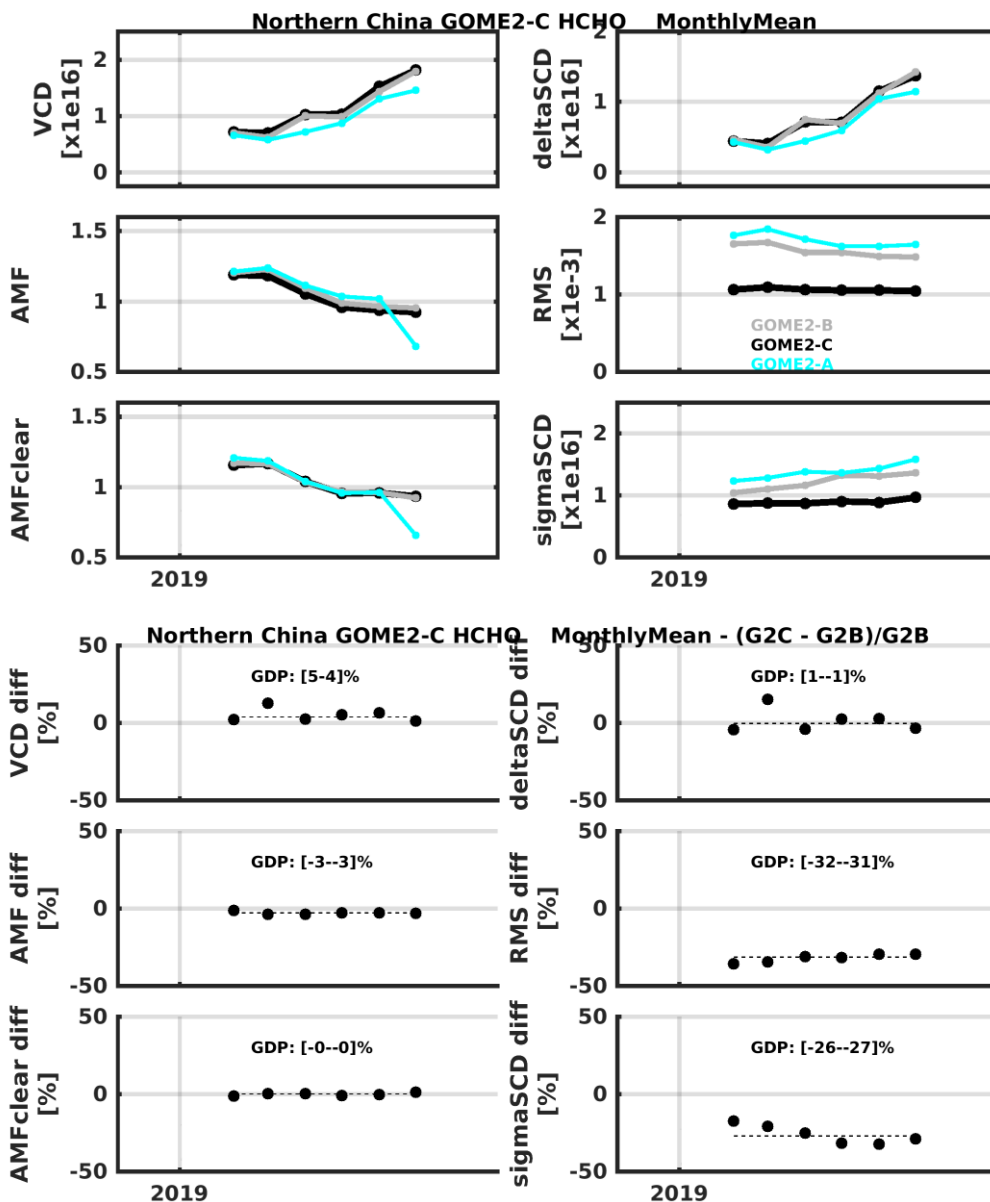


Figure D.2: same as Figure D.1, but for the Northern China region.

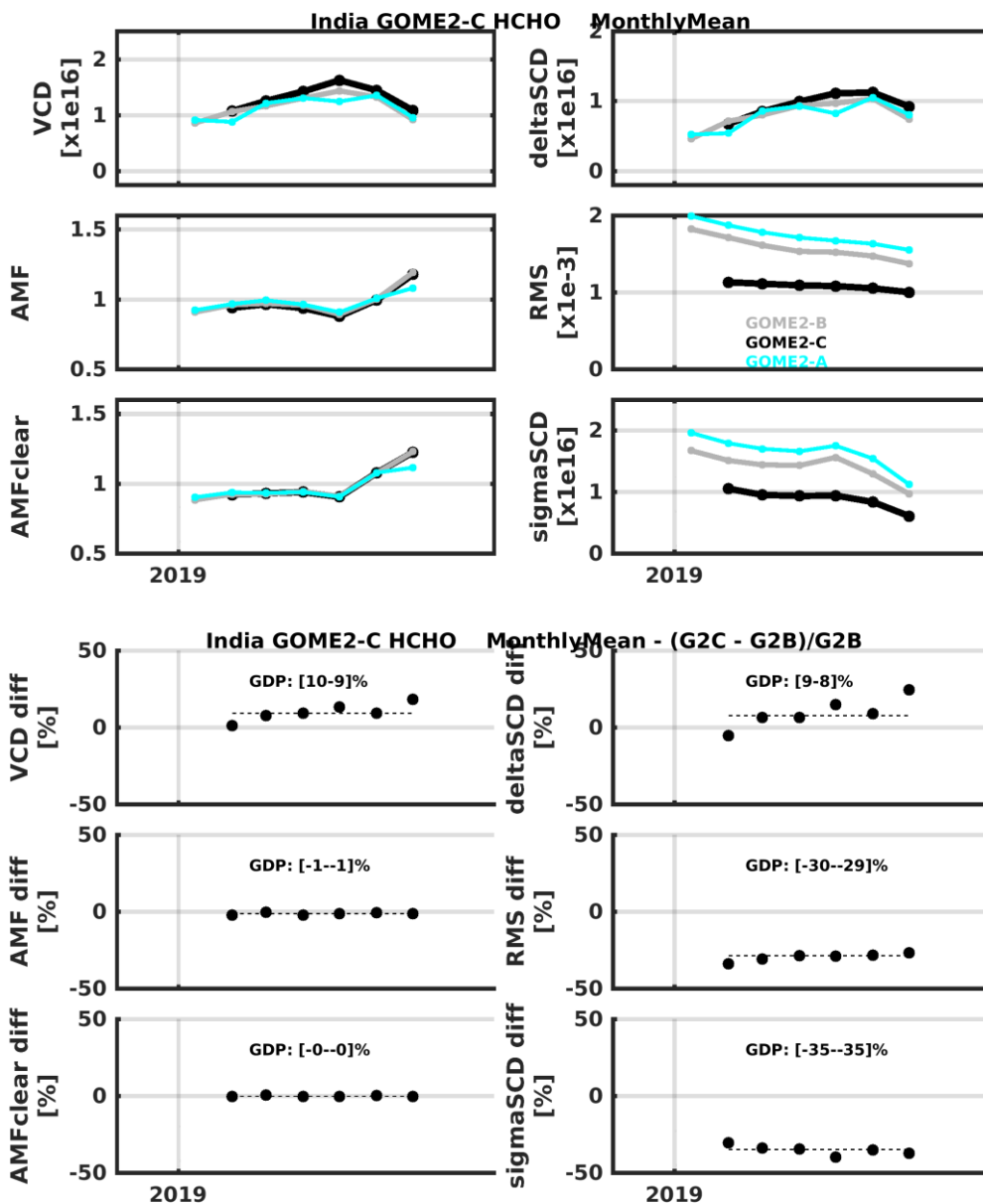


Figure D.3: same as Figure D.1, but for the India region.

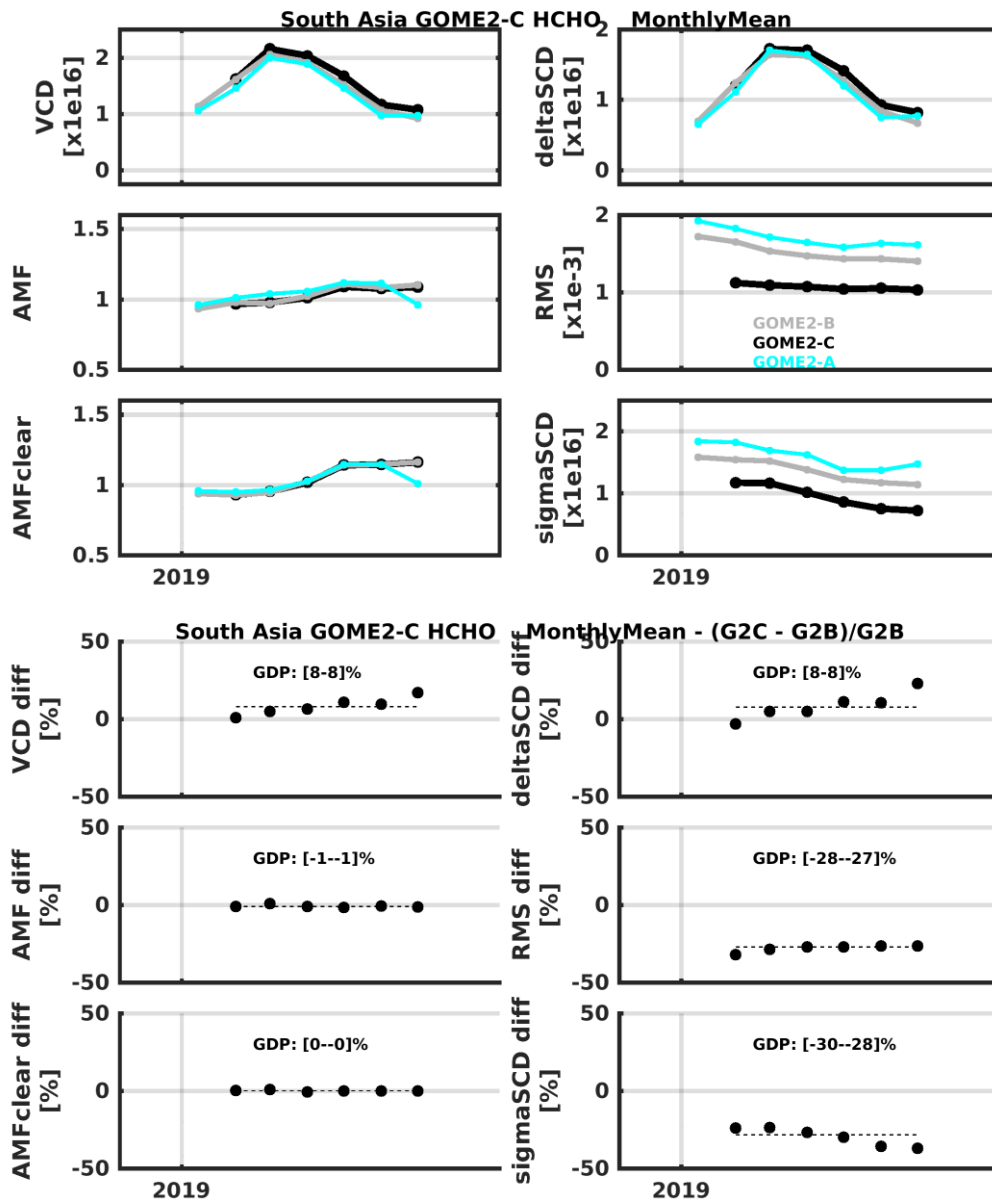


Figure D.4: same as Figure D.1, but for the Southern Asia region.

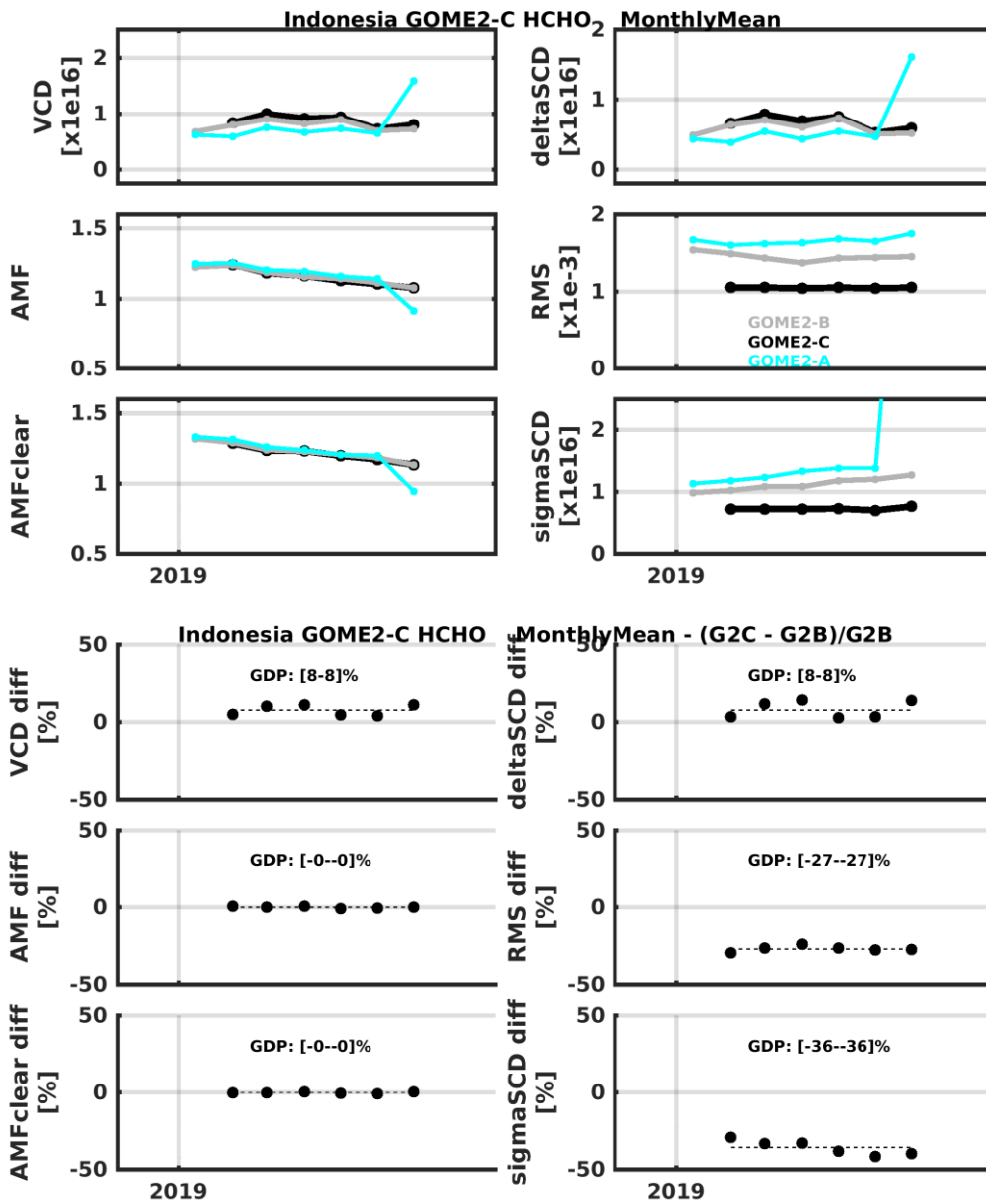


Figure D5: same as Figure D.1, but for the Indonesia region.

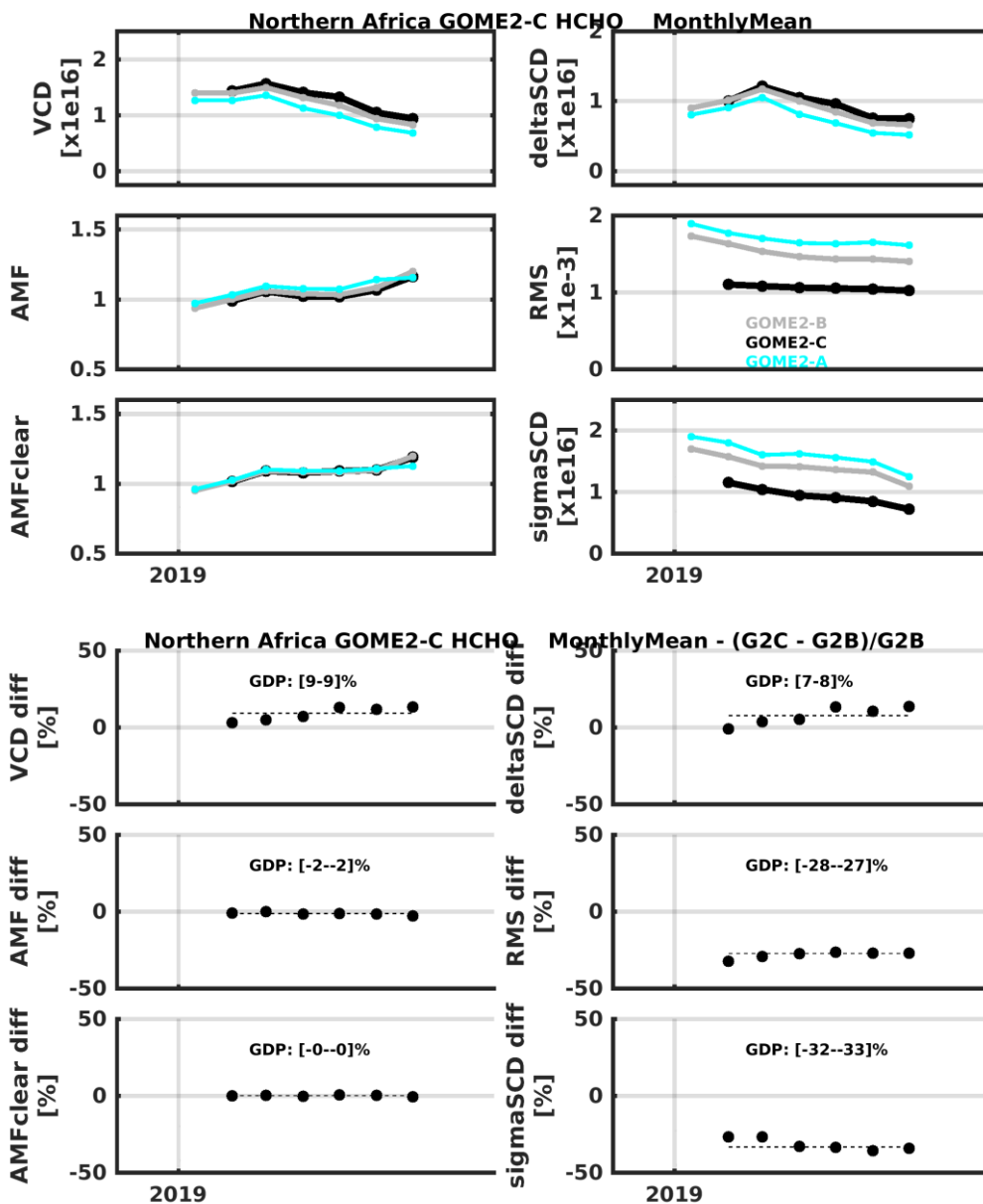


Figure D.6: same as Figure D.1, but for the Northern Africa region.

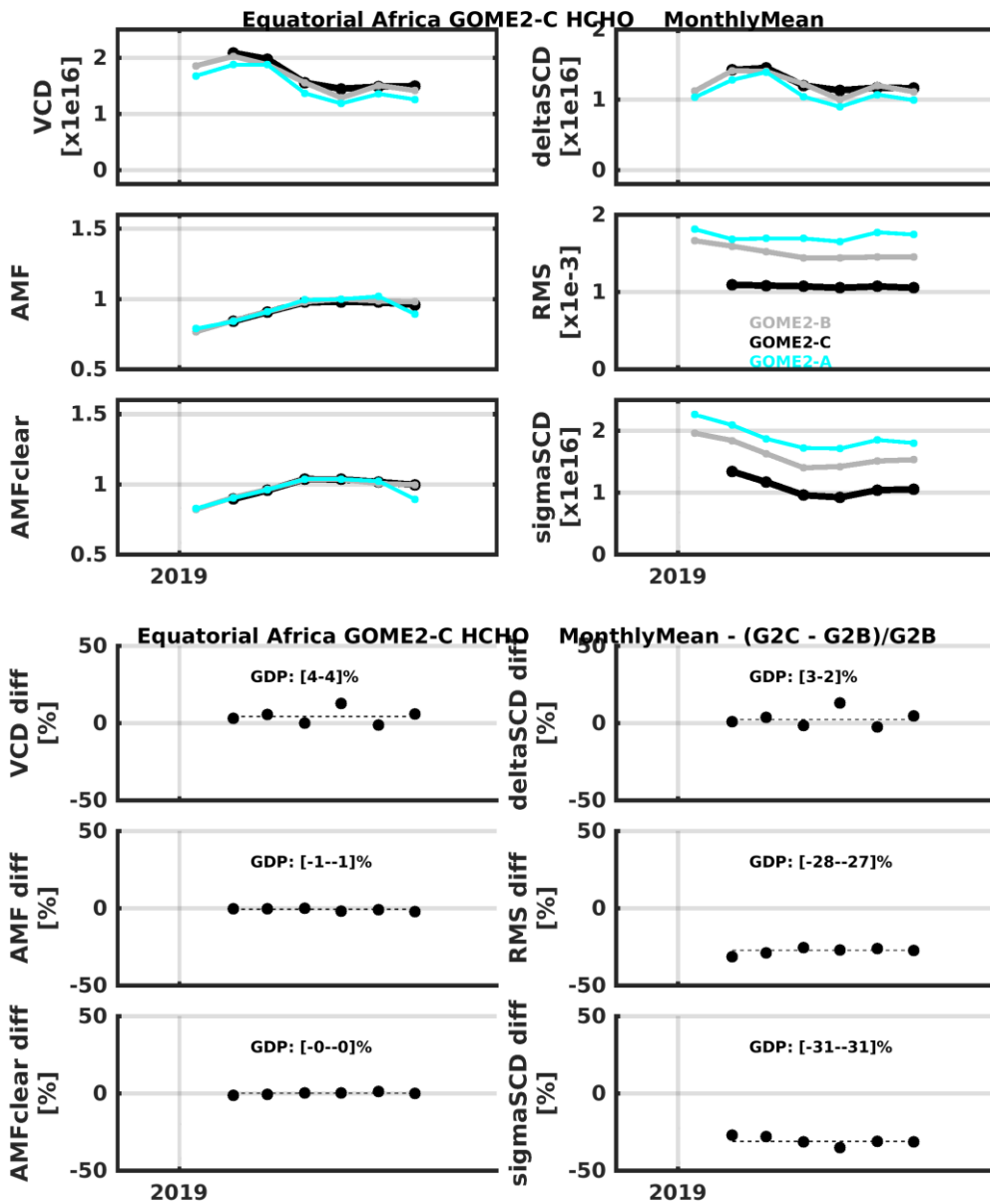


Figure D.7: same as Figure D.1, but for the Equatorial Africa region.

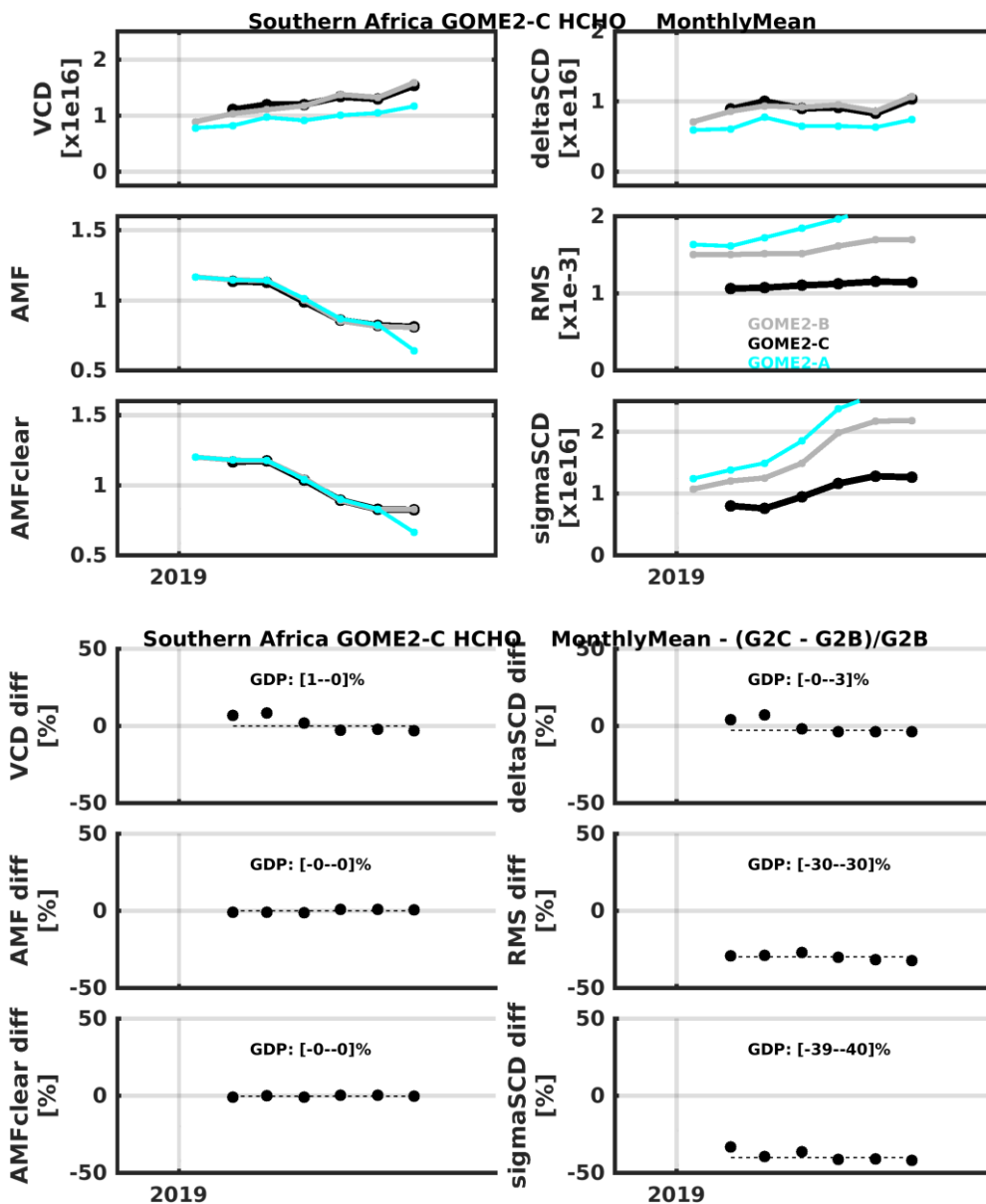


Figure D.8: same as Figure D.1, but for the Southern Africa region.

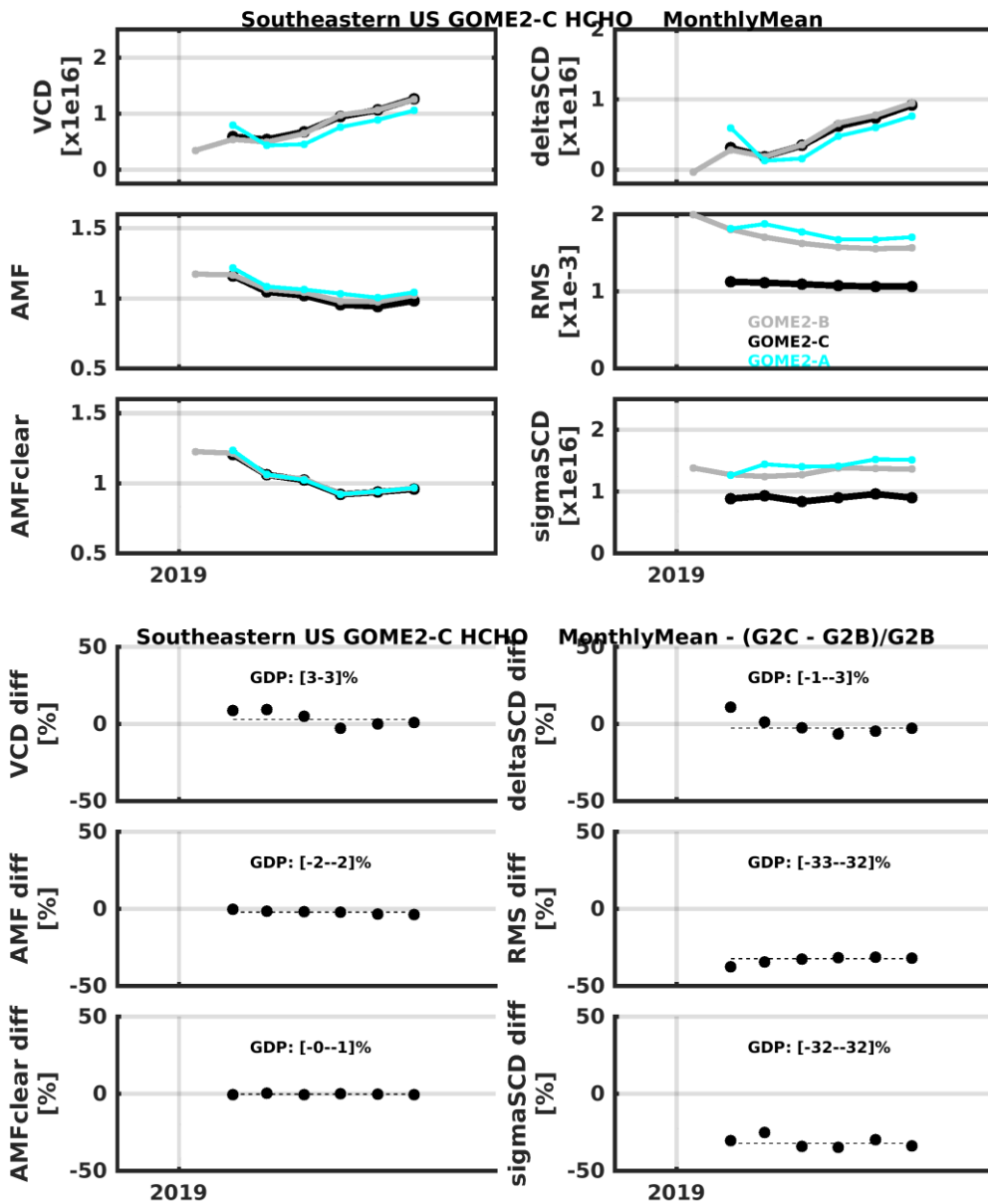


Figure D.9: same as Figure D.1, but for the Southeastern US region.

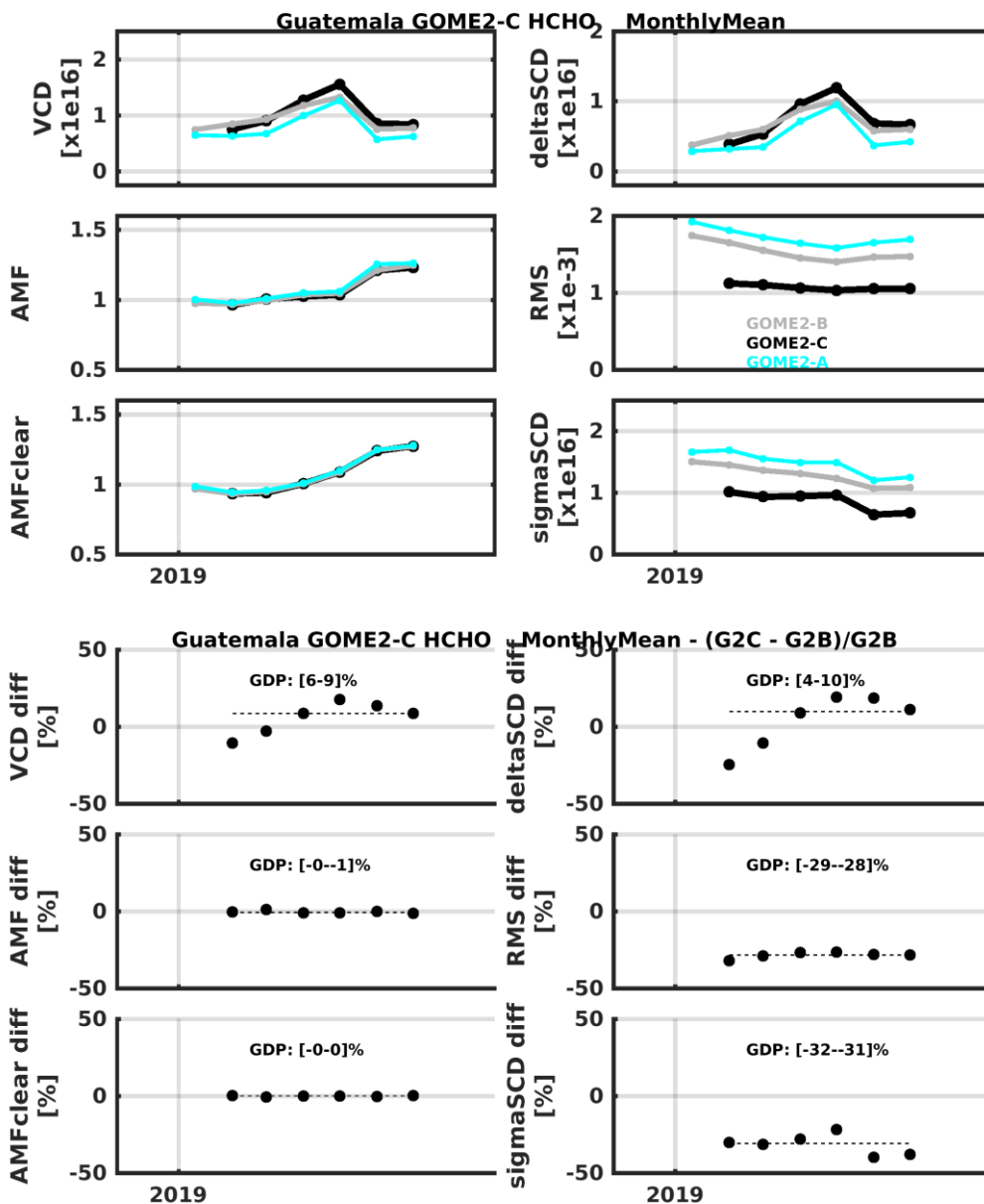


Figure D.10: same as Figure D.1, but for the Guatemala region.

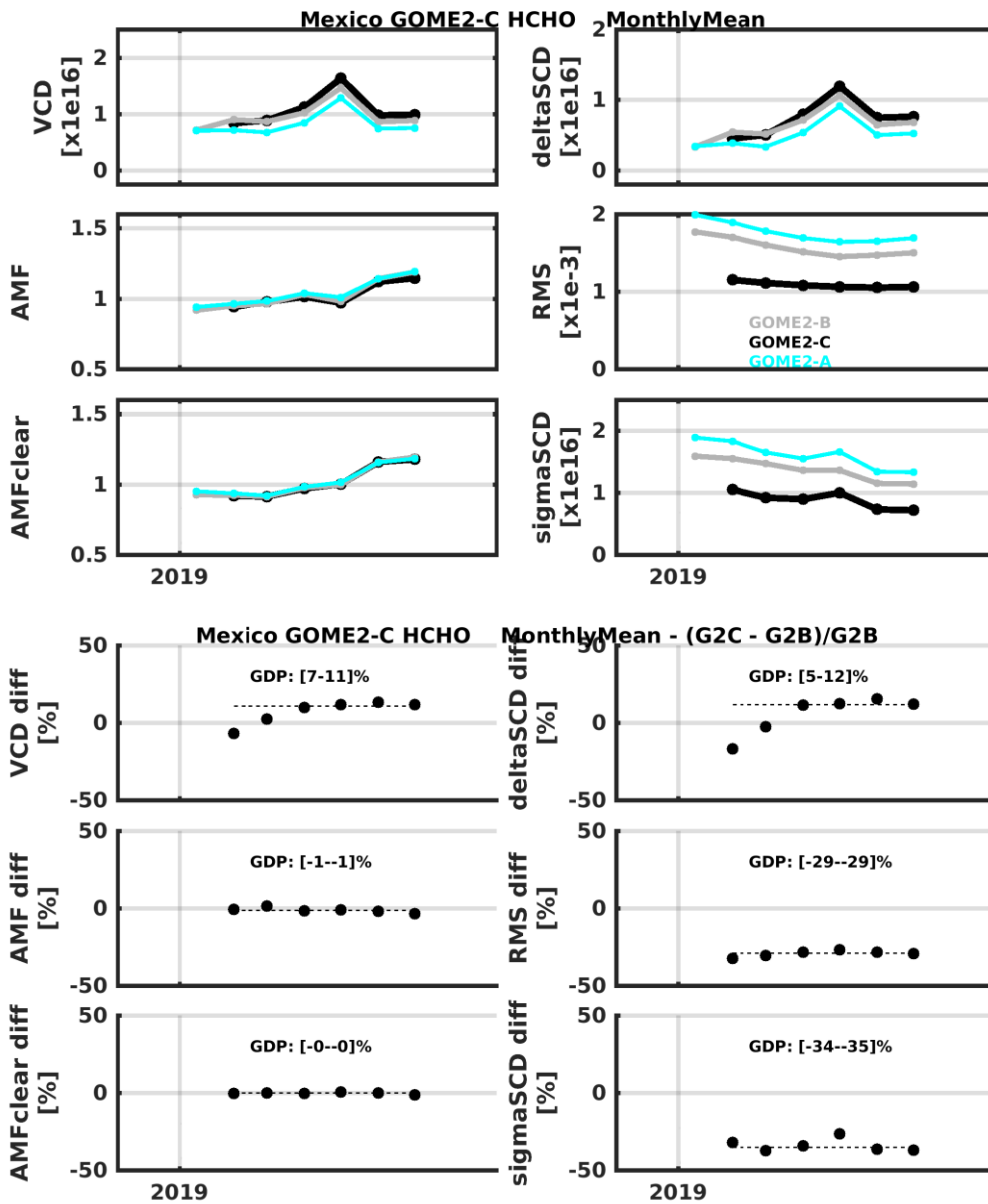


Figure D.11: same as Figure D.1, but for the Mexico region.

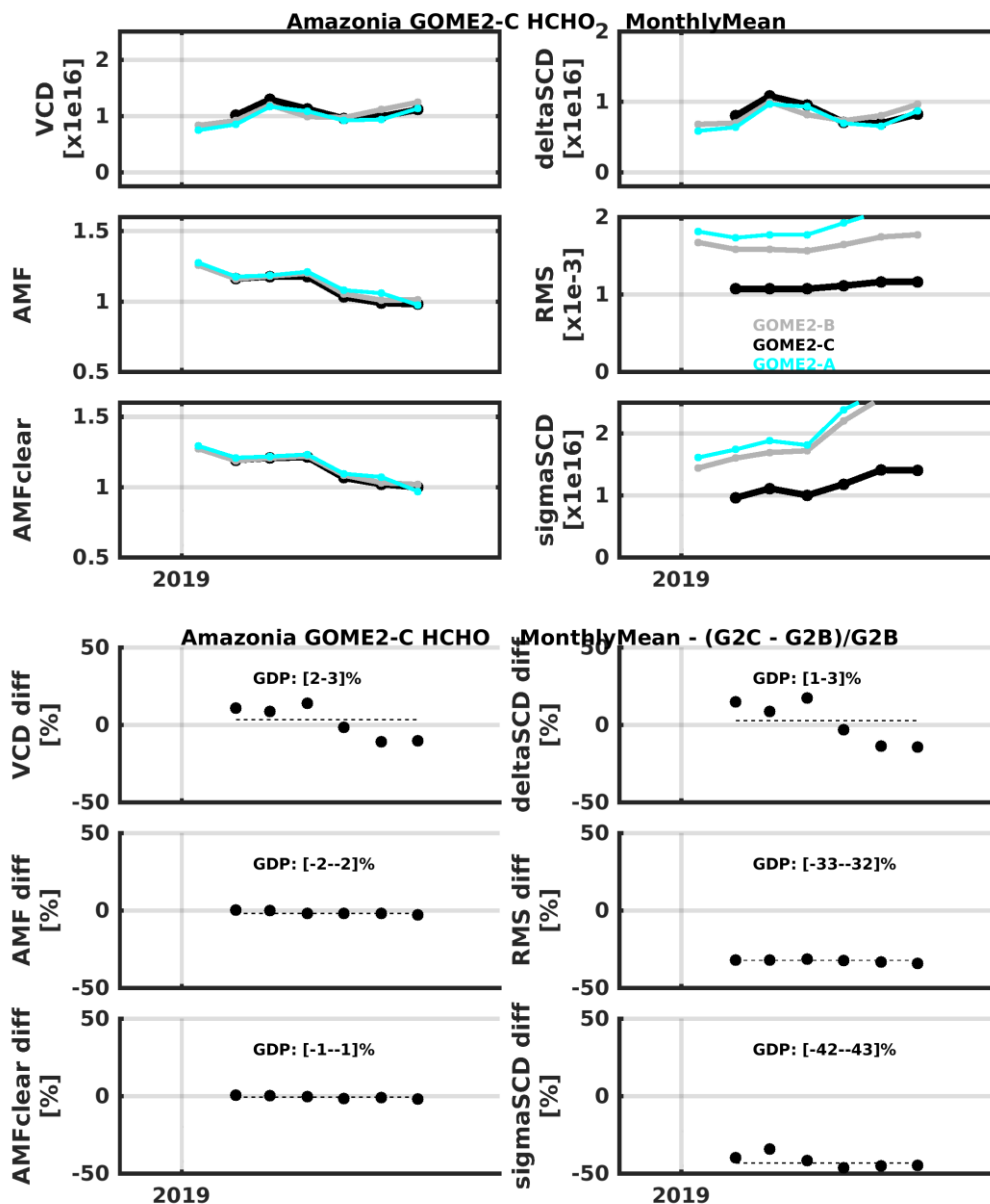


Figure D.12: same as Figure D.1, but for the Amazonia region.

Table D.2: Mean and median VCD differences in [%] between GOME-2C and GOME-2B over the different regions.

regions	(G2C-G2B)/G2B Mean and median VCD differences:
Amazonia	[2; 3]%
Equatorial Africa	[4; 4]%
Guatemala	[6; 9]%
India	[10; 9]%
Indonesia	[8; 8]%
Mexico	[7; 11]%
Northern Africa	[9; 9]%
Northern Australia	[3; 1]%

Northern China	[5; 4]%
Northern India	[9; 8]%
South Asia	[8; 8]%
Southeastern US	[3; 3]%
Southern Africa	[1; 0]%
Southern China	[15; 15]%
Equatorial Pacific	[-5; -5]%
Pacific	[-2; -2]%
Europe	[-22; -13]%

The quality of the GOME-2C results is good, with values comparable to those of GOME-2B for the different emission regions investigated here, with maximum mean differences of 15% in VCD, as summarized in Table D.2. GOME-2A values are generally smaller than GOME-2B/C, probably as a result of both degradation and smaller pixels. GOME-2C is generally a few % larger than GOME-2B in emission regions (up to 15% in mean over Southern China), while in regions with low HCHO, GOME-2C is slightly smaller (Pacific and Europe in winter time). RMS values for GOME-2C are comparable with values of GOME-2A and GOME-2B at the beginning of their mission ($\sim 1e-3$), and smaller than current RMS values (effect of degradation).

E. COMPARISON WITH GROUND-BASED MEASUREMENTS

In this section, GOME-2B and GOME-2C HCHO vertical column densities (VCDs) are compared to correlative ground-based observations, as done in previous Validation Report and Operation Reports, but extending the correlative ground-based dataset to MAXDOAS and FTIR datasets from the NIDFORVAL project.

E.1. Ground-based correlative data

Figure E.1 illustrates the FTIR and MAXDOAS stations coming from the NIDFORVAL project that are used in this study. These datasets cover a wide range of HCHO levels, with Arctic (Ny Alesund, Kiruna, Sodankyla), oceanic (La Reunion Maito, Lauder), mountainous (Jungfrauoch) remote levels to polluted conditions (St Petersburg, Bremen, Paris, Toronto, Xianghe, Uccle, Mainz, Thessaloniki, Madrid, Chiba, Vallejo and Unam) and large HCHO columns (Porto Velho).

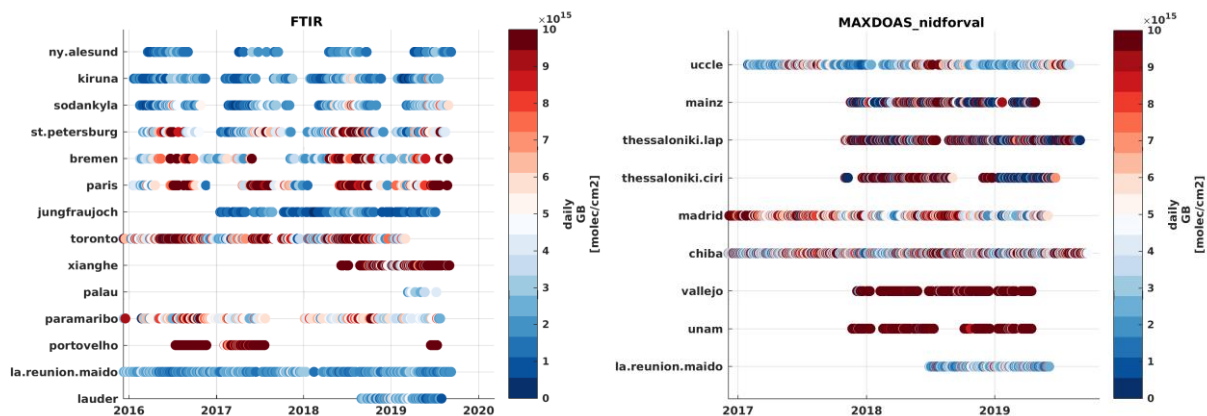


Figure E1: Time-series of available ground-based data for the validation of GOME-2C HCHO data. The 2 figures are color-coded with their respective HCHO VCD values.

Information about the FTIR dataset can be found in Vigouroux et al. (2018).

E.2. Validation method

The validation is done as previously done for MAXDOAS in Validation Report for GDP 4.8 (AC SAF VR 2015) and for FTIR as presented in Pinardi et al. (2018).

Satellite HCHO VCD daily means are calculated using all pixels falling within a radius of 150 km around the stations and meeting the following selection criteria:

- HCHO slant column densities (SCDs) larger than 4×10^{16} molec/cm², solar zenith angle (SZA) lower than 70°, and cloud fraction lower than 40%.

For the ground-based data, daily means are performed for FTIR (due to their sometimes limited number of direct-sun solar measurements in one day), while MAXDOAS data are averaged for data within +/- 1h of the satellite overpass time.

In order to allow direct comparison between GOME-2 and ground-based observations, the difference in vertical sensitivity between both measurement types is taken into account by applying the satellite column averaging kernels to the ground-based HCHO profiles when available (i.e. for the FTIR dataset). Smoothed ground-based HCHO VCDs ($VCD_{GB,smoothed}$) are derived for each day by averaging retrieved ground-based profiles falling within the time-selection and convolving the mean profile (x_{GB}) with the corresponding satellite column averaging kernel (AK_{sat}):

$$\text{VCD}_{\text{GB,smoothed}} = \text{AK}_{\text{sat}} * \mathbf{x}_{\text{GB}}$$

If the first altitude level of the satellite column averaging kernel is above the altitude of the station, then the averaging kernel is extrapolated down to the altitude of the station.

E.3. Comparison with MAXDOAS

One example of comparison results (HCHO VCD time-series and corresponding scatterplots) for Uccle MAXDOAS is shown in Figure E.2. Uccle and Reunion-Maido are the only BIRA stations measuring during Feb-July 2019 and considering the limited time-period (6 months) results at Uccle are similar to what obtained in the past Operation Reports (Op.Rep. 2019a) for GOME-2B and GOME-2A.

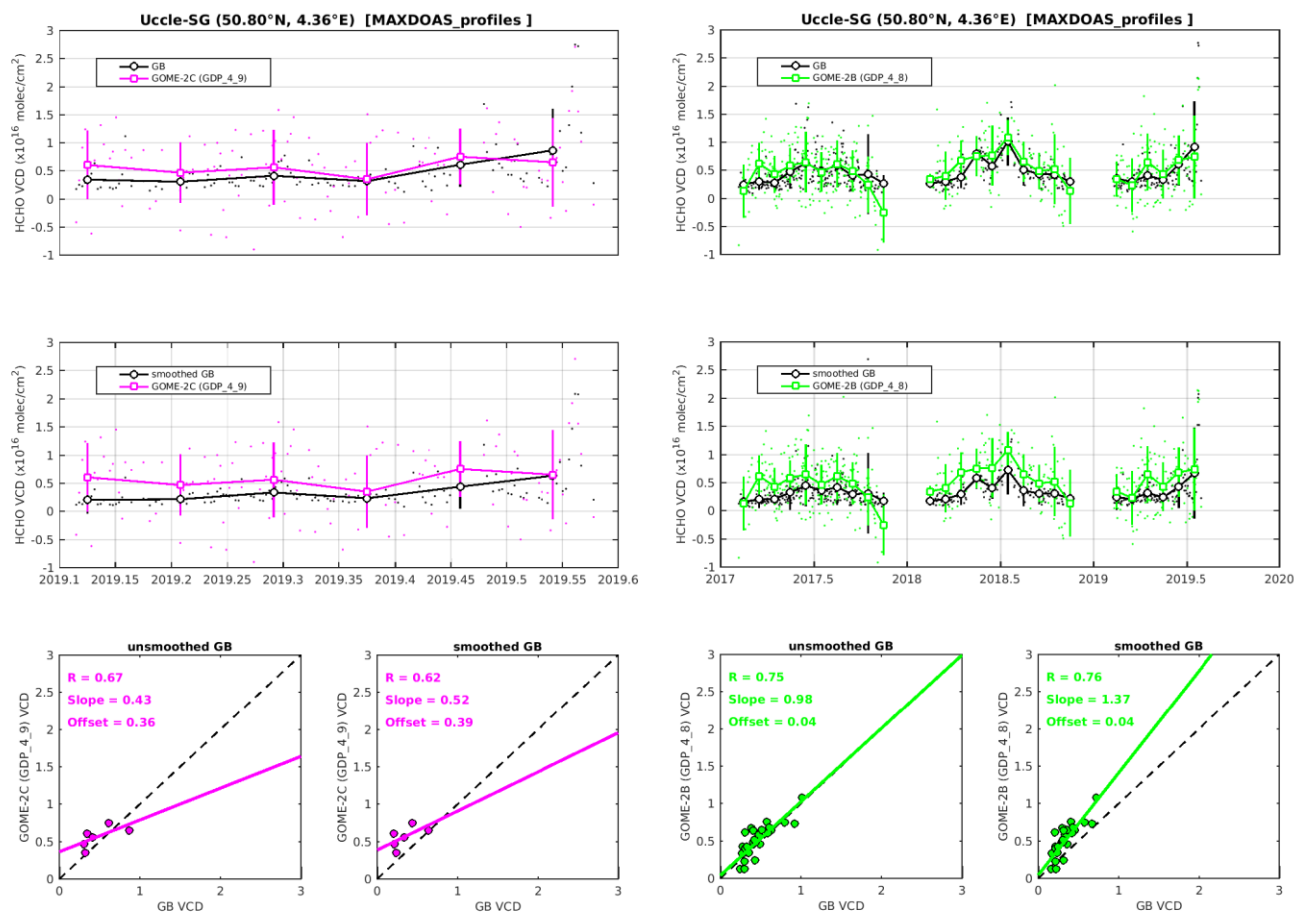


Figure E2: Comparison between GOME-2 (left: GOME-2C, right: GOME-2B) and smoothed and unsmoothed MAX-DOAS HCHO VCDs at Uccle. HCHO VCDs time-series appear in the upper (unsmoothed MAX-DOAS) and mid (smoothed MAX-DOAS) plots while the lower plots correspond to the scatterplots where VCDs are expressed in 10^{16} molec/cm².

Seven additional MAXDOAS stations coming from the NIDFORVAL project have been used to assess GOME-2 data, only focusing on the original VCD_{GB} data, without considering the MAXDOAS profiles. The comparisons at the nine stations are presented in Figure E.3 under the form of overview scatterplots of daily points for GOME-2C and GOME-2B (in the period Feb to July 2019). Similar results are obtained for both satellites with respect to the MAXDOAS data ensemble. Thessaloniki_ciri and Thessaloniki_lap report a large number of negative VCD columns for 2019, which needs more in-depth verification (currently on-going by the AUTH data providers), and these stations are thus excluded from the rest of the

analysis. In addition, at Unam and Vallejo Mexican stations, ground-based data are much larger than both GOME-2 satellites, which was also seen within the TROPOMI validation study (Vigouroux et al., 2019, Milano conference). Only one month of data is available at those sites at the time of the analysis, and these are not considered in the monthly comparisons of Figure E4. From Figure E3, an evident conclusion is the larger spread (especially in the negative values) of the GOME-2C columns, compared to GOME-2B results. This was already seen in the verification sections C.1 and C.2, where figure C.1.2 and C.2.2) presented a viewing dependence in the GOME-2C data, leading to high HCHO values in the nadir pixels and lower values for the large scan angles for the HCHO VCD, coming from the slant columns. This was also seen by the Bremen team, that could not propose a better solution for the GOME-2C HCHO analysis (Richter et al., 2019).

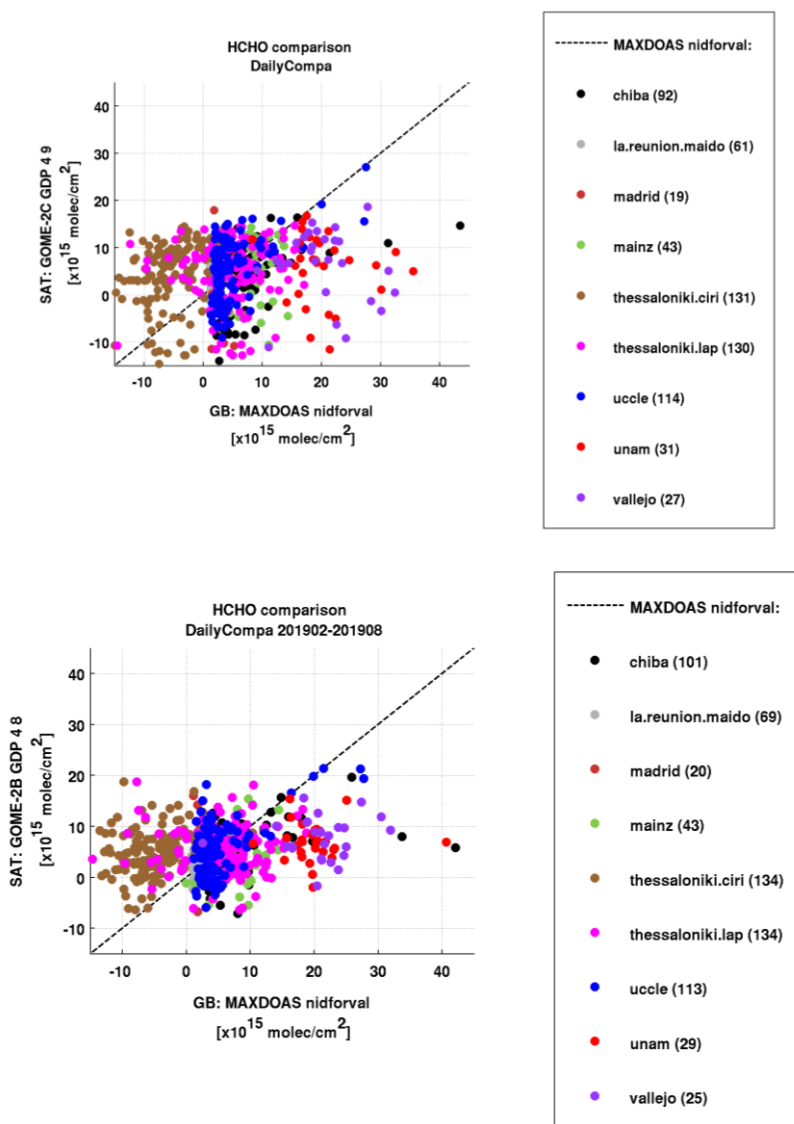


Figure E3: Scatter plots between daily GOME-2 (top: GOME-2C, bottom: GOME-2B) and MAXDOAS HCHO VCDs at 9 stations over the period February to July 2019.

On the other side, when performing monthly mean comparisons (Figure E.4), the ensemble of points lies between 0 and 10×10^{15} molec/cm² around the 1-1 line, with correlation around 0.5 and slopes between 0.5 and 0.6. Slopes smaller than 1 are to be expected as the MAXDOAS does not see HCHO above the first few km and the MAXDOAS and satellite have very different vertical sensitivity (see figure E6). expected as Similar results for the statistical analysis are thus found for these limited GOME-2B and GOME-2C datasets.

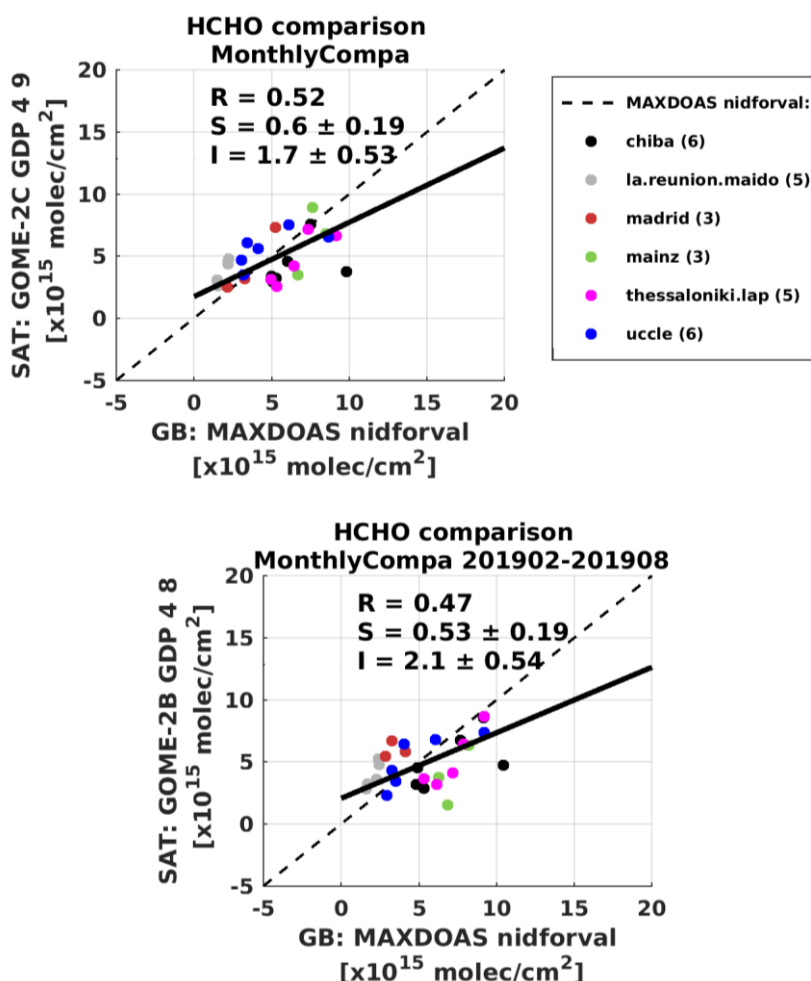


Figure E4: Scatter plots between monthly GOME-2 (top: GOME-2C, bottom: GOME-2B) and MAXDOAS HCHO VCDs at 9 stations over the period February to July 2019.

E.4. Comparison with FTIR

One example of comparison results (HCHO VCD time-series and corresponding scatterplots) for Xianghe FTIR is shown in Fig. E.5. Xianghe is an interesting site, in a suburban area, where the FTIR has been installed in 2018 and where a BIRA MAXDOAS is also installed since 2010 (having instrumental issues for the past year) and was used in comparisons in past validation report (AC SAF VR 2015) and Operation Reports. As discussed for the MAXDOAS comparisons, larger negative spread is found for GOME-2C, which is not as strongly present in GOME-2B results. As can be seen in Figure E.5, ground-based FTIR is larger than both GOME-2 data, but taking into account the difference in sensitivity (and smoothing the FTIR profile with GOME-2 averaging kernels), the comparison slightly improves. It should be noted that the MAXDOAS results at the same station are much more sensitive to the impact of smoothing (cf Op. Rep. 2018, Figure 7.20), due to the different sensitivities between MAXDOAS and FTIR column averaging kernels (see Figure E.6 as an illustration).

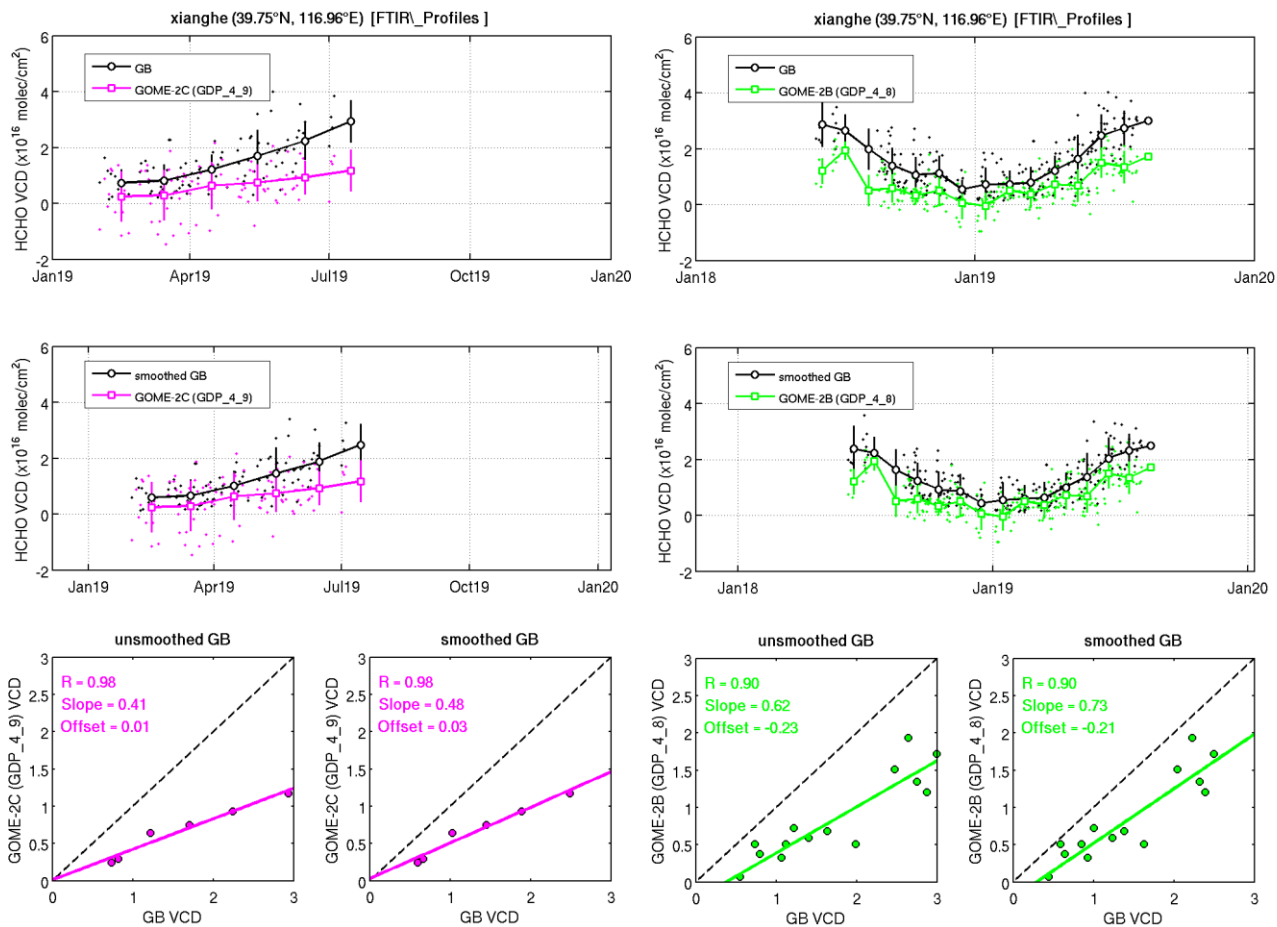


Figure E5: Comparison between GOME-2 (left: GOME-2C, right: GOME-2B) and smoothed and unsmoothed FTIR HCHO VCDs at Xianghe. HCHO VCDs time-series appear in the upper (unsmoothed MAX-DOAS) and mid (smoothed MAX-DOAS) plots while the lower plots correspond to the scatterplots where VCDs are expressed in 10^{16} molec/cm².

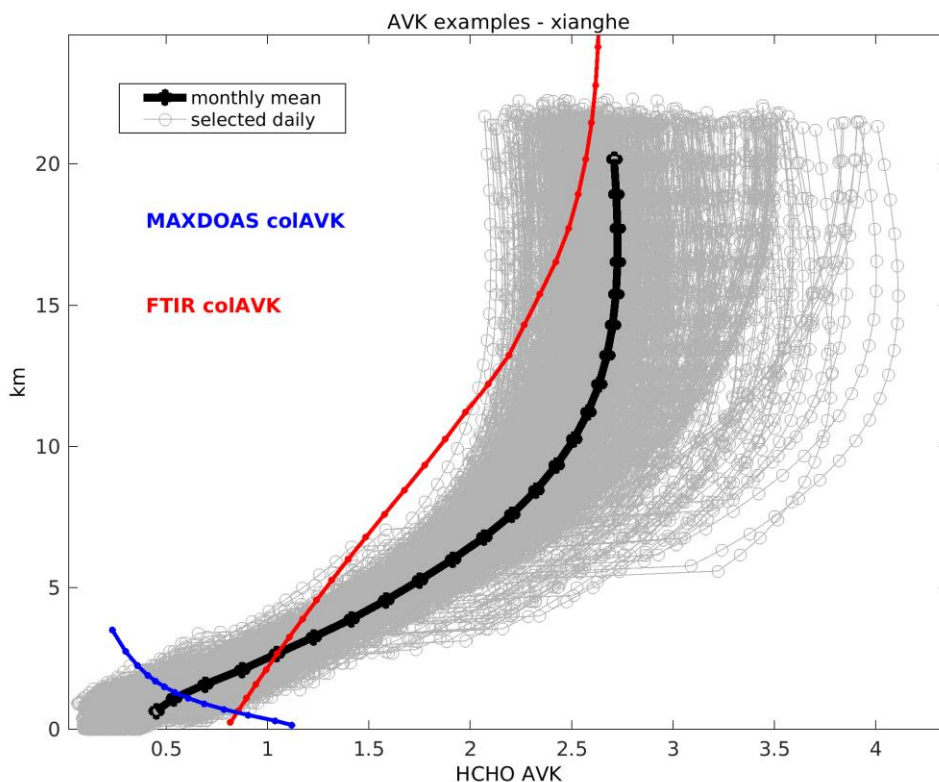


Figure E6: Example of averaging kernels typical behavior for GOME-2, FTIR and MAXDOAS HCHO in Xianghe station.

When grouping the results of the 14 FTIR stations in one overview scatter plot for the daily comparisons (Figure E7), the large spread in the GOME-2C (negative) values is clear. This is strongly reduced in the monthly mean comparisons (Figure E8), but the differences with the GOME-2B results are clear: for similar correlations (around 0.65 and 0.7 for the original and the smoothed comparisons), the slopes of GOME-2C are much smaller than those for GOME-2B: about 0.47 and 0.56 (original and smoothed FTIR) compared to 0.8 and 0.94. It should however be mentioned that the statistical regression analysis is strongly sensitive to the large HCHO columns, as coming from the Xianghe FTIR data.

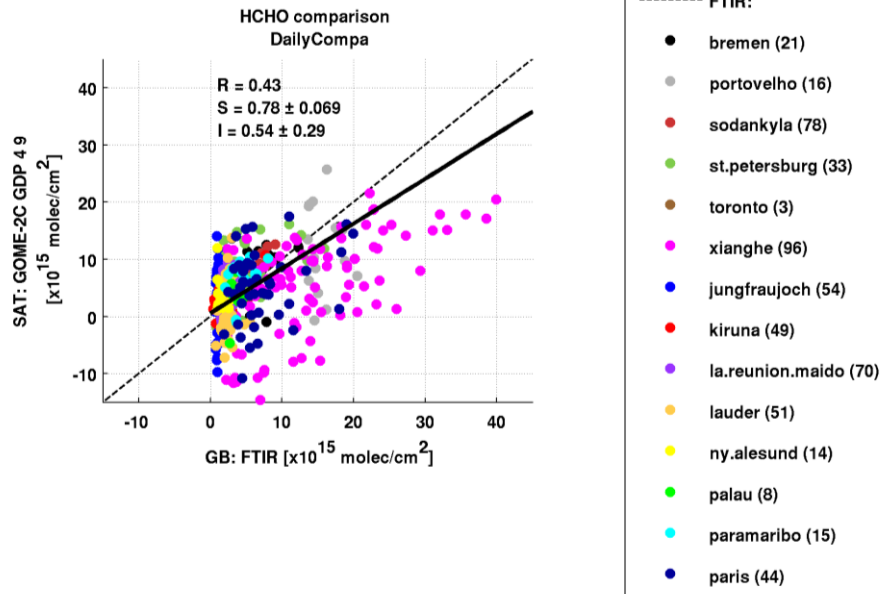


Figure E7: Scatter plots between GOME-2 and FTIR HCHO VCDs at 14 stations.

FTIR	GOME-2C	GOME-2B [201902-201907]
Monthly with original FTIR	<p>HCHO comparison MonthlyCompa</p> <p>SAT: GOME-2C GDP 4.9 [x10¹⁵ molec/cm²]</p> <p>GB: FTIR [x10¹⁵ molec/cm²]</p> <p>R = 0.66 S = 0.47 ± 0.068 I = 2.4 ± 0.35</p> <p>----- FTIR:</p> <ul style="list-style-type: none"> ● bremen (5) ● portovelho (2) ● sodankyla (5) ● st.petersburg (4) ● toronto (1) ● xianghe (6) ● jungfrauoch (6) ● kiruna (5) ● la.reunion.maido (5) ● lauder (4) ● ny.alesund (4) ● palau (4) ● paramaribo (6) ● paris (6) 	<p>HCHO comparison MonthlyCompa 201902-201908</p> <p>SAT: GOME-2B GDP 4.8 [x10¹⁵ molec/cm²]</p> <p>GB: FTIR [x10¹⁵ molec/cm²]</p> <p>R = 0.64 S = 0.8 ± 0.12 I = -0.16 ± 0.55</p> <p>----- FTIR:</p> <ul style="list-style-type: none"> ● bremen (5) ● portovelho (2) ● sodankyla (5) ● st.petersburg (5) ● toronto (1) ● xianghe (6) ● jungfrauoch (6) ● kiruna (5) ● la.reunion.maido (6) ● lauder (4) ● ny.alesund (4) ● palau (3) ● paramaribo (6) ● paris (6)
Monthly with smoothed FTIR	<p>HCHO column comparison MonthlyCompa</p> <p>SAT: GOME-2C GDP 4.9 [x10¹⁵ molec/cm²]</p> <p>GB: smoothed FTIR [x10¹⁵ molec/cm²]</p> <p>R = 0.72 S = 0.56 ± 0.068 I = 2 ± 0.33</p> <p>----- smoothed FTIR:</p> <ul style="list-style-type: none"> ● bremen (5) ● portovelho (2) ● sodankyla (5) ● st.petersburg (4) ● toronto (1) ● xianghe (6) ● jungfrauoch (6) ● kiruna (5) ● la.reunion.maido (5) ● lauder (4) ● ny.alesund (4) ● palau (4) ● paramaribo (6) ● paris (6) 	<p>HCHO column comparison MonthlyCompa 201902-201908</p> <p>SAT: GOME-2B GDP 4.8 [x10¹⁵ molec/cm²]</p> <p>GB: smoothed FTIR [x10¹⁵ molec/cm²]</p> <p>R = 0.69 S = 0.94 ± 0.12 I = -0.9 ± 0.54</p> <p>----- smoothed FTIR:</p> <ul style="list-style-type: none"> ● bremen (5) ● portovelho (2) ● sodankyla (5) ● st.petersburg (5) ● toronto (1) ● xianghe (6) ● jungfrauoch (6) ● kiruna (5) ● la.reunion.maido (6) ● lauder (4) ● ny.alesund (4) ● palau (3) ● paramaribo (6) ● paris (6)

Figure E7: Scatter plots between GOME-2 and FTIR HCHO VCDs at 14 stations.

E.5. Conclusion on ground-based comparisons

Although the reported comparisons only covers 6 months of data, and more investigation should be performed with 1 year of data, including an assessment of the impact of vertical sensitivity for MAXDOAS stations, including ground-based data coming from the side project NIDFORVAL allowed to perform a first analysis of GOME-2C (and GOME-2B) HCHO VCD values. Clear differences in the daily comparisons (both for MAXDOAS and FTIR data) are found for GOME-2C compared to results with GOME-2B. The large daily spread in the GOME-2C (with a larger number of more negative columns) pointed out in the verification Section C, is also seen in the validation exercise. The impact of the large GOME-2C spread is reduced in the monthly mean comparisons but differences in the monthly comparisons is found for the FTIR exercise. Slope of 0.56 wrt smoothed FTIR values are found for GOME-2C, compared to 0.94 with GOME-2B. Validation results with FTIR are thus at the limit of the 50% threshold requirement for GOME-2C.

F. CONCLUSIONS AND PERSPECTIVES

This document reports on the interim verification of AC-SAF GOME-2C HCHO column data products retrieved at DLR with versions 4.9 of the GOME Data Processor (GDP), using level-1B-R1 data based on level-0-to-1B processor version 6.3. HCHO column data are compared to Metop-B GOME-2 HCHO results and to correlative MAXDOAS and FTIR ground-based data.

The following main conclusions can be drawn:

1. The current quality of the MetOp-C GOME-2 radiance and irradiance spectra in the 328.5-346 nm spectral interval enables HCHO slant column retrievals. However, a viewing geometry dependence is found in GOME-2C SCD and SCDcorrected, that is transferred in the VCD, leading to a large number of negative columns for large off-nadir scan angles. This dependence might be due to polarisation-related spectral features in the level-1 data.
2. GOME-2C HCHO fit residuals and scatter on the slant column are systematic smaller than for GOME-2B, in a range from 20% in tropical to 50% over high latitudes, but are generally comparable to those obtained from Metop-B spectra at beginning of operations. GOME-2C slant columns show a slightly higher bias compared to GOME-2B.
3. A smaller signature of the SAA is found for GOME-2C compared to MetopB.
4. GOME-2C VCD are about ~71% larger than GOME-2B for the pixels between 70°S and 70°N, with VCD values exceeding 10^{15} molecules/cm², and excluding the SAA regions. If only pixels exceeding 6×10^{15} molecules/cm² VCD are considered, the average difference is within 32%. In the explored emissions regions, the temporal evolution of GOME-2C is similar to GOME-2B, with GOME-2C being generally a few % larger than GOME-2B in emission regions (up to 15% in average over Southern China), while in regions with low HCHO, GOME-2C is slightly smaller (Pacific and Europe in winter time).

In average, these differences meets the accuracy requirement of HCHO for polluted cases (50%), and are very close to the optimal requirement (30%).

5. Gathering of preliminary HCHO columns from ground-based MAXDOAS (9 stations) and 14 FTIR stations within the NIDFORVAL project allowed a first validation of the GOME-2C and GOME-2B vertical columns. Differences in the daily comparisons (both for MAXDOAS and FTIR data) are found for GOME-2C compared to results with GOME-2B, with a larger daily spread in the first case (with a larger number of large negative columns), as already pointed out in the verification section. The impact of the large GOME-2C spread values is reduced in the monthly mean comparisons and similar results are found for the MAXDOAS comparisons, while larger differences are found for the FTIR case. Slope of 0.56 wrt smoothed FTIR values are found for GOME-2C, compared to 0.94 with GOME-2B. Validation results present a relatively good agreement, but the FTIR comparisons over 6 months are at the limit of the 50% threshold requirement for GOME-2C.

Future improvement of the operational product could be obtained on all GOME-2 instruments by implementing outcomes of the latest scientific GOME-2 algorithm versions (QA4ECV product and S5p prototype) into the UPAS operational processor. This would include an improved reference sector correction (to account for the east/west dependency), Earthshine as reference and a spike removal algorithm.

G. REFERENCES

G.1. Applicable documents

- [ATBD] Algorithm Theoretical Basis Document - GOME-2 Total Column Products of Ozone, NO₂, BrO, HCHO, SO₂, H₂O, OClO, and Cloud Properties (GDP 4.8 for AC SAF OTO and NTO), Valks, P., Loyola D., Hao N., Hedelt, P., Slijkhuis S., Gross, M., Gimeno Garcia, S., Lus, R., 2017, https://acsaf.org/docs/atbd/Algorithm_Theoretical_Basis_Document_NTO_OTO_DR_GDP48_Jun_2017.pdf
- [PUM] Valks, P., et al., (2017), Product User Manual for GOME Total Column Products of Ozone, NO₂, BrO, HCHO, SO₂, H₂O, OClO and Cloud Properties, GDP 4.8, SAF/AC/DLR/PUM/01, Iss. 3/A, Rev. 2, June, 2017, https://acsaf.org/docs/pum/Product_User_Manual_NTO_OTO_DR_GDP48_Jun_2017.pdf
- [PRD] Service Specification Document, SAF/AC/FMI/RQ/SESP/001/issue 1.3, Hovila, J., Hassinen, S., 17 June 2019, https://acsaf.org/docs/AC_SAF_Service_Specification.pdf
- [VIM] Joint Committee for Guides in Metrology (JCGM/WG 2) 200:2008 & ISO/IEC Guide 99-12:2007, International Vocabulary of Metrology – Basic and General Concepts and Associated Terms (VIM), <http://www.bipm.org/en/publications/guides/vim.html>
- [GUM] Joint Committee for Guides in Metrology (JCGM/WG 1) 100:2008, Evaluation of measurement data – Guide to the expression of uncertainty in a measurement (GUM), http://www.bipm.org/utis/common/documents/jcgm/JCGM_100_2008_E.pdf
- [QA4EO] A Quality Assurance framework for Earth Observation, established by the CEOS. It consists of ten distinct key guidelines linked through an overarching document (the QA4EO Guidelines Framework) and more community-specific QA4EO procedures, all available on <http://qa4eo.org/documentation.html> A short QA4EO "user" guide has been produced to provide background into QA4EO and how one would start implementing it (http://qa4eo.org/docs/QA4EO_guide.pdf)

G.2. Reference

G.2.1 Peer-reviewed articles

- Boersma, K. F., Eskes, H. J. and Brinksma, E. J.: Error analysis for tropospheric NO₂ retrieval from space, *J. Geophys. Res.*, 109(D4), doi:10.1029/2003JD003962, 2004.
- Brion, J., et al.: Absorption spectra measurements for the ozone molecule in the 350-830 nm region, *J. Atmos. Chem.*, 30, 291-299, 1998.
- Chance, K. and Kurucz, R. L.: An improved high-resolution solar reference spectrum for earth's atmosphere measurements in the ultraviolet, visible, and near infrared, *J. Quant. Spectrosc. Radiat. Transf.*, 111(9), 1289-1295, 2010.
- De Smedt, I., Müller, J.-F., Stavrou, T., van der A, R., Eskes, H. and Van Roozendael, M.: Twelve years of global observations of formaldehyde in the troposphere using GOME and SCIAMACHY sensors, *Atmos. Chem. Phys.*, 8(16), 4947-4963, 2008.

- De Smedt, I., Stavrakou, T., Müller, J. F., van Der A, R. J. and Van Roozendael, M.: Trend detection in satellite observations of formaldehyde tropospheric columns, *Geophys. Res. Lett.*, 37(18), L18808, doi:10.1029/2010GL044245, 2010.
- De Smedt, I., Long-Term Global Observations of Tropospheric Formaldehyde Retrieved from Spaceborne Nadir UV Sensors, Ph.D. thesis, Faculty of Applied Sciences, University of Brussels, Belgium, 2011.
- Fleischmann, O. C., et al.: New ultraviolet absorption cross-sections of BrO at atmospheric temperatures measured by time-windowing Fourier transform spectroscopy, *J. Photochem. Photobiol. A*, 168, 117–132, 2004.
- Kleipool, Q. L., Dobber, M. R., de Haan, J. F. and Levelt, P. F.: Earth surface reflectance climatology from 3 years of OMI data, *J. Geophys. Res.*, 113(D18), D18308, doi:10.1029/2008JD010290, 2008.
- Koelemeijer, R. B. A., Stammes, P., Hovenier, J. W. and de Haan, J. F.: A fast method for retrieval of cloud parameters using oxygen A band measurements from the Global Ozone Monitoring Experiment, *J. Geophys. Res.*, 106(D4), 3475-3490, doi:10.1029/2000JD900657 2001.
- Koelemeijer, R. B. A., de Haan, L. H. and Stammes, P.: A database of spectral surface reflectivity in the range 335 – 772 nm derived from 5 years of GOME observations, *J. Geophys. Res.*, 108(D2), doi:10.1029/2002JD002429, 2003.
- Kurosu, T. P., OMHCHO README FILE, http://www.cfa.harvard.edu/~tkurosu/SatelliteInstruments/OMI/PGEReleases/READMEs/OMHCHO_README.pdf, 2008.
- Lutz, R., D. Loyola, S. Gimeno Garcia, and F. Romahn, OCRA radiometric cloud fractions for GOME-2A/B, *Atmos. Meas. Tech.*, 9, 2357-2379, 2016.
- Meller, R., and Moortgat, G. K.: Temperature dependence of the absorption cross section of HCHO between 223 and 323K in the wavelength range 225–375 nm, *J. Geophys. Res.*, 105(D6), 7089–7102, doi:10.1029/1999JD901074, 2000.
- Palmer, P. I., Jacob, D. J., Chance, K. V., Martin, R. V., D, R. J., Kurosu, T. P., Bey, I., Yantosca, R. and Fiore, A.: Air mass factor formulation for spectroscopic measurements from satellites: Application to formaldehyde retrievals from the Global Ozone Monitoring Experiment, *J. Geophys. Res.*, 106(D13), 14539-14550, doi:10.1029/2000JD900772, 2001.
- Platt, U. and Stutz, J.: *Differential Optical Absorption Spectroscopy: Principles and Applications (Physics of Earth and Space Environments)*, Springer-Verlag, Berlin, Heidelberg, ISBN 978-3540211938, 2008.
- Pukite, J., Köhl, S., Deutschmann, T., Platt, U. and Wagner, T.: Extending differential optical absorption spectroscopy for limb measurements in the UV, *Atmos. Meas. Tech.*, 3(3), 631-653, doi:10.5194/amt-3-631-2010, 2010.
- Rozanov, A., Rozanov, V., and Burrows, J. P.: A numerical radiative transfer model for a spherical planetary atmosphere: Combined differential integral approach involving the Piccard iterative approximation, *J. Quant. Spectrosc. Radiat. Transfer*, 69, 491–512, 2001.
- Spurr, R. J. D.: LIDORT and VLIDORT: Linearized pseudo-spherical scalar and vector discrete ordinate radiative transfer models for use in remote sensing retrieval problems, in *Light Scattering Reviews*, edited by A. Kokhanovsky, pp. 229–271, Berlin, 2008.
- Vandaele, A.C., et al.: High-resolution Fourier transform measurement of the NO₂ visible and near-infrared absorption cross-section: Temperature and pressure effects, *J. Geophys. Res.*, 107, D18, 4348, doi:10.1029/2001JD000971, 2002.
- Veefkind, J. P., Aben, I., McMullan, K., Förster, H., de Vries, J., Otter, G., Claas, J., Eskes, H. J., de Haan, J. F., Kleipool, Q., van Weele, M., et al.: TROPOMI on the ESA Sentinel-5 Precursor: A GMES mission for global observations of the atmospheric composition for climate, air quality and ozone layer applications, *Remote Sensing of Environment*, 120(0), 70-83, 2012.
- Vigouroux, C., C. A. B. Aquino, M. Bauwens, C. Becker, T. Blumenstock, M. De Mazière, O. Garcia, M. Grutter, C. Guarin, J. Hannigan, F. Hase, N. Jones, R. Kivi, D. Koshelev, B. Langerock, E. Lutsch, M. Makarova, J.-M. Metzger, J.-F. Müller, J. Notholt, I. Ortega, M. Palm, C. Paton-Walsh, A. Poberovskii, M. Rettinger, J. Robinson, D. Smale, T. Stavrakou, W. Stremme, K. Strong, R. Sussmann, Y. Té, and G. Toon: NDACC harmonized formaldehyde time-series from 21

FTIR stations covering a wide range of column abundances, *Atmos. Meas. Tech.*, 11, 5049-5073, 2018.

- Vountas, M., Rozanov, V. V. and Burrows, J. P.: Ring effect: impact of rotational Raman scattering on radiative transfer in earth's atmosphere, *J. of Quant. Spec. and Rad. Trans.*, 60(6), 943-961, 1998.

G.2.2 Technical notes and presentations

- O3M SAF validation Report, Validation report of GOME-2NRT, offline and reprocessed GDP 4.8 HCHO column data for MetOp-A and B, 2015.
https://acsaf.org/docs/vr/Validation_Report_NTO_OTO_DR_HCHO_GDP48_Oct_2015.pdf
- O3M SAF validation Report, Offline Total Formaldehyde (O3M-10 OTO HCHO) GOME-2, H2CO, 2010, http://o3msaf.fmi.fi/docs/vr/Validation_Report_OTO_HCHO_Feb_2010.pdf.
- De Smedt, I., T. Stavrakou, J.-F. Müller, N. Hao, et al., H₂CO columns retrieved from GOME-2: first scientific results and progress towards the development of an operational product, Proceedings of the 2009 EUMETSAT Meteorological Satellite Conference, Bath, U.K., 2009.
- Callies, J., Corpaccioli, E., Eisinger, M., Hahne, A., and Lefebvre, A.: GOME-2- Metop's second-generation sensor for operational ozone monitoring, *ESA Bull.*, 102, 28–36, 2000.
- Dikty, S. and Richter, A.: GOME-2 on MetOp-A Support for Analysis of GOME-2 In-Orbit Degradation and Impacts on Level 2 Data Products, Final Report, Version 1.2 - Issue Date: 14.10.2011.
- Lacan, A. and Lang, R.: Investigation on GOME-2 throughput degradation, Final report, EUM/LEO/REP/09/0732 Issue 1.1, 16. July 2011.
- Lang, R., Munro, R., Livschitz, Y., Dyer, R., and Lacan, A.: GOME-2 FM3 Long-Term In-Orbit Degradation - Basic Signatures After 2nd Throughput Test, EUMETSAT Technical report, EUM.OPS-EPS.DOC.09.0464, 2009.
- Munro, R., Eisinger, M., Anderson, C., Callies, J., Corpaccioli, E., Lang, R., Lefebvre, A., Livschitz, Y., and Albinana, A. P.: GOME-2 on MetOp, Proc. of The 2006 EUMETSAT Meteorological Satellite Conference, Helsinki, Finland, 2006.
- Operation Reports (Op.Rep. 2019a): OPERATIONS REPORT, Issue 1/2019, Reporting period: January –June 2019, https://acsaf.org/docs/or/AC_SAF_Operations_Report_1-2019.pdf, Sept 2019.
- Pinardi, G., C. Vigouroux, M. Van Roozendaal, F. Hendrick, I. De Smedt, M. De Mazière, A. Richter, E. Peters, F. Wittrock, A. Piters, T. Wagner, S. Donner, U. Frieb, T. Drosoglou, A. Bais, S. Wang, A. Saiz-Lopez, H. Irie, T. Blumenstock, F. Hase, C. Guarin, W. Stremme, J. W. Hannigan, I. Ortega, N. B. Jones, R. Kivi, Y. Té, E. Lutsch, K. Strong, M. Makarova, J. Notholt, M. Palm, M. Rettinger, R. Sussmann, D. Smale, Validation of GOME-2 AC SAF GDP HCHO columns using ground-based MAXDOAS and FTIR column measurements, oral presentation at the EUMETSAT conference, 17 to 21 September 2018, Tallin, Estonia.
- Pinardi, G., Michel Van Roozendaal, François Hendrick, Steven Compernelle, Jean-Christopher Lambert, Jose Granville, Cléo Gielen, Alexander Cede, Yugo Kanaya, Hitoshi Irie, Folkard Wittrock, Andreas Richter, Enno Peters, Thomas Wagner, Julia Remmers, Udo Friess, Tim Vlemmix, Ankie Piters, Martin Tiefengraber, Jay Herman, Nader Abuhassan, Robert Holla, Alkis Bais, Dimitris Balis, Theano Drosoglou, Natalia Kouremeti, Jari Hovila, J. Chong, Oleg Postlyakov, Alexander Borovski, Jianzhong Ma, Satellite nadir NO₂ validation based on direct-sun and MAXDOAS network observations, oral presentation at the DOAS workshop, September 2017, Yokohama, Japan.
- Richter, A., T. Bösch, S. Noel, M. Weber, H. Bovensmann, J. Burrows, Evaluation of GOME2C L1 quality using non-operational L2 retrievals, Presentation at GSAG #53, EUMETSAT, 20 May 2019.
- Siddans et al.: Analysis of GOME-2 Slit function Measurements: Final Report Eumetsat Contract No. EUM/CO/04/1298/RM, 2006.

- Vigouroux, C., Langerock, B., Pinardi, G., and the FTIR and DOAS NIDFORVAL teams, Validation of TROPOMI/S5P HCHO measurements using UV-Vis DOAS and FTIR ground-based networks, presentation at the Living Planet symposium, 10-13 May 2019, Milano, Italy.